Non-linear Analysis of Reinforced Concrete Deep Beams using Finite Element Method

A thesis submitted for partial fulfillment of the requirements of the degree of M.Sc. in structures

by

LOUAY MAHMOUD ABDEL WAHAB

Department Of Civil Engineering
Faculty of Engineering & Architecture
University of Khartoum, Sudan

Supervisor:

PROFFESOR/ ABU BAKAR ABDEL WAHAB MOHAMMED

March 2004

Abstract

The purpose of this thesis is to analyze reinforced concrete deep beams in linear, non-linear and ultimate ranges. The finite element method is utilized to study the behavior of deep beams under monotonically increasing loads. All the major factors causing material non-linearity are considered.

Primary consideration is given to the representation of shear transfer mechanisms, due to aggregate interlock in cracked concrete and the dowel action in reinforcement. Expressions are derived from an analytical model in conjunction with experimental data to provide shear stress and stiffness values for special elements used to model the aggregate interlock mechanism. These are expressed as function of crack width, concrete strength and shear displacement. A comparable approach is used to derive expression for the dowel action mechanism. This is expressed in terms of the reinforcement diameter, yield stress, dowel displacement and crushing strength of concrete.

The bond-slip phenomenon between concrete and reinforcement is accounted for by using non-dimensional spring element. Stiffness values for such elements are obtained from expression based on experimental data.

Improved isoparametric quadrilateral elements and triangular elements are used to represent concrete. Material response is assumed to be orthotropic with tangent stiffness E_1, E_2 derived from stress-strain relation for concrete under a general biaxial state of stress.

The reinforcement is represented in a discrete manner. One- dimensional flexural elements and axial ones are used for this purpose. Material response is assumed to be elastic-perfectly plastic.

Two methods of cracking representation are used: the discrete cracking approach and distributed cracking approach.

The computer program with combined incremental-iterative method is used to solve the non-linear problem.

The results of this investigation gave good agreement with conclusion reached by the task committee 426 on shear and diagonal tension[1] ,that in reinforced concrete deep beams bond-slip mechanism takes the major part of shear transfer while the other mechanisms(aggregate interlock and dowel action) take less part. This is indicated by comparing the results of this investigation with experimental results obtained by isreal[2].

Acknowledgement

Iwould like to thank **professor/Abu baker Abdal Wahab** for his support, constructive criticism and sincere follow up throughout the study and preparation of this thesis.

And also I would like to thank teaching assistant/Asim Elsanosi for his giving good idea about the content of this thesis.

Table of Content

Page No.

CHAPTER(1)
INTRODUCTION

1.1 General

Reinforced concrete deep members often form part of a more complex structural system in multi-story buildings. They commonly take the form of shear walls , deep beams , corbels , bracket, and other configurations. The rapid increase in the number of tall buildings for both residential and commercial purposes has necessitated the search for analytical methods to achieve improved understanding of the behavior of structural components in such buildings.

The main factor affecting the diffinition of deep beams is span-depth ratio $[\frac{L}{H}]$ or $[\frac{l_n}{d}]$ where L and L_n are span and clear span of deep beam and H,d are depth and effective depth of deep beam . *ACI* code stipulates that a beam can be considered deep if $[\frac{l_n}{d}] < 5$. Euro-international concrete committee decided that a beam could

be considered deep if $[\frac{L}{H}]$<2 or 2.5 for simply supported and continuous beams respectively.

some investigator have decided that the shear span-depth ratio$[\frac{a}{d}]$ is more meaningfull to define a deep beam, and that a beam could be considered deep if $[\frac{a}{d}]$<2.5.

The distribution of stresses in vertical section in deep beams(non-linear distribution) significantly deviates from that of shallow beams(straight line distribution).This property was one of the important factors for classifing deep beams such that deep beam may be defined as beam whose bending stresses deviate appreciably from the straight line distribution assumed in elementary beam theory (the normal theory of flexure based on Navier-Bernoully principles is not applicable).For this reason the ordinary beam design methods to calculate the member strength are inapplicable in case of deep beams.

A meaningful analysis of reinforced concrete deep beams requires an analytical model which reproduces the behavior of the member as accurately as possible. some of difficulties encountered in analytical studies of the behavior of deep beams arise from the following:

- The nonhomogeneous nature of construction.
- Material response to load is non-linear.
- The non-linearity of the stress-strain relationship for concrete.
- The continuously changing topology of concrete due to cracking.
- Experimental evidence indicates that the relation between bond stress and bond-slip is non-linear.

Recent development of the finite element method of analysis permits consideration of members which are non homogeneous, defined by irrigular bounderies, arbitrarily supported and loaded. The method is used to determine the internal stresses and displacement for reinforced concrete members subjected to progressively increasing load,with recognition for several sources of non-linearity. The resulting model permits accounting for

- The influence of reinforcement.
- Changing topology due to progressive cracking.
- Realistic bond stress transfer between concrete and reinforcement.

Incremental loading permits study of member behavior throught the entire range from zero to ultimate loads.

1.2 Thesis Outlines:

A literature survey is presented in chapter (2) summarizing the current knowledge related to experimental and analytical previous work in reinforced concrete deep beams . The behavior of reinforced concrete deep beams under different type of loading including the effect of web reinforcement, span/depth ratio, shear span/depth ratio, concrete strength and other factors related to shear capacity is studied.

In this research an analytical model based on experimental results of Dulaska[3] and Fenwick Paulay[4] is used to simulate dowel action and aggregate interlock mechanisms this work is described in chapter(3). In these models a dowel bar is treated as beam on elastic foundation while aggregate interlock is modeled by idealization of irregulasr crack surface. Linkage elements are employed to model these mechanisms by releasing the pairs of node defined along discrete crack when cracking is detected.

This investigation also explores various finite element models in order to achieve the non-linear behavior of reinforced concrete deep beam. All the sources of non-linearity mentioned in chapter (4) are accounted for. A discretized system consisting of plane stress elements and one-dimensional elements, modeling the concrete and reinforcement, respectively, is constructed for analysis. The plane stress elements used are improved isoparametric quadrilateral elements. The main reinforcement is represented by one-dimensional flexural elements while one-dimensional axial elements are used to model the web reinforcement. Elastic-perfectly plastic material response is assumed for steel. Special emphasis is placed on the representation of cracking and modeling of the post-cracking shear transfer mechanism. The members are assumed to be acted upon by monotonically increasing live loads. Two methods of crack modeling are considered as mentioned in chapter (4): distributed cracking approach and discrete cracking approach. In some cases the use of discrete cracking is sufficient. In other cases the use of discrete cracking in conjunction with distributed cracking approach proved to be necessary if a realistic prediction of a member's response is sought.

A constitutive relation for concrete based on the analytical and experimental investigations of Lui and Tasuji is used to describe the behavior of concrete under a different state of stresses as mentioned in chapter (5).

The computer program with a combined incremental-iterative numerical method is used to solve the non-linear problem. This consists of applying the external load in a number of increments. Specified number of iterations to bring mount of equilibrium

violation to a tolerable limit follows each load increment. The stiffness matrix is updated at the beginning of each load increment. Convergence of solution checked by either the nodal displacement criterion or the unbalanced load criterion.

The validity of the proposed finite element models is tested by comparing the results obtained from analysis with the corresponding experimental ones as mentioned in chapter(6).

CHAPTER (2)
LIRERATURE REVIEW

The research investigation of shear strength of reinforced concrete deep beams is divided into two parts: experimental investigation supported by statistical correlation's to get shear capacity equation fitting the experimental data, and analytical investigation using finite element to simulate the non-linearity and cracking of concrete.

2.1 Review of Experimental Investigation

De Pavia and Siess[5],described an experimental investigation on the shear strength and behavior of some moderately reinforced concrete deep beams by loading these beams at third points .

The main factors considered in this investigation are:

Amount of tension reinforcement.

Concrete strength.

Amount of web reinforcement.

Span-depth ratio.

They concluded that for reinforced concrete deep beams without web reinforcement there is a high load capacity beyond the diagonal cracking and that the addition of vertical stirrup and inclined bars have little effect on the ultimate strength .Also they showed the fact that the concrete strength had no effect on the ultimate strength of beams failing in flexure.

Gergely[6] performed an experimental model to study the contribution of aggregate interlock and dowel action to post cracking shear capacity of reinforced beams with no web reinforcement. Gergely estimated contribution of aggregate iterlock to be 40% to 60% of the total shear and that of dowel action was estimated to be 20% to 25% of the total shear. It was also concluded that the dowel action is the main factor causing splitting along main reinforcement in beam without web reinforcement.

Taylor[7] conducted several experiments to investigate the effect of aggregate interlock and dowel action by studying the factors affecting the two mechanisms.

To simulate the aggregate interlock Taylor used two types of specimens:

- Block tests.
- Beam tests.

The main factors included in these tests to study their influences in aggregate interlock mechanism are:

1- The displacement ratio Δ_N/Δ_S, where Δ_N is the displacement normal to the crack (crack width), and Δ_S is the horizontal displacement (shear displacement).

2- Concrete strength.

3- Aggregate size.

4- Aggregate type.

The block test has the advantage that it requires less sophisticated set-up and measuring devices, and is also more economic and consumes less time than the beam test. But the beam test is useful in obtaining more reliable results about aggregate interlock mechanism.

For dowel action mechanism Taylor considered the following factors:

1- Concrete strength.

2- Shear span.

3- Crack width.

4- Concrete cover.

The main purpose of this work was to establish complete dowel load-displacement curves, and to estimate the contribution of shear resisting mechanism in reinforced concrete beam without web reinforcement.

Their results were as follows:

Compression zone	20 - 40%
Aggregate interlock	33 - 50%
Dowel action	15 - 25%

Paulay and Loeber[8], concluded that the crack width is the most important factor affecting the aggregate interlock shear stiffness and that the aggregate shape and size had very little influence on shear stress-displacement relationships.

Kong et al[9],performed an experimental investigation to study the effect of different percentage of web reinforcement in thirty five normal weight concrete deep beams. The beams were tested under two-point loading. It was found that the effectiveness of

various web reinforcement depended on the span/depth ratio [$\frac{L}{H}$] and clear shear span/depth ratio[$\frac{a}{d}$]. for low [$\frac{L}{H}$] and [$\frac{a}{d}$] ratios, horizontal web reinforcement gave the best results.

Another detailing of web reinforcement was studied experimentally and reported by Kong et al[11] consisting of inclined bars. He found that web reinforcement was an effective type of reinforcement to increase shear strength of reinforced concrete deep beams and also to control deflection and cracking.

Kong and Robins[11],carried out tests on simply supported light weight concrete deep beams, and they developed an equation that calculates the ultimate load for normal weight concrete deep beams. This equation is not necessarily suitable for normal weight concrete beams.

Further experimental work on lightweight concrete deep beams was reported by Kong and Robins[12]. They revised their previous equation in two factors: the [$\frac{a}{d}$] ratio explicitly allowed for, and they used concrete cylinder splitting tensile strength , f_t ,as they though that the concrete contribution to the ultimate shear strength is much more directly related to f_t than cylinder compressive strength f_c. Their tests showed that the clear shear span/depth ratio [$\frac{a}{d}$] had greater effect on cracking and ultimate loads than span/depth ratio [$\frac{L}{H}$].

Smith and Vantsiotis[13]carried out tests for simply supported reinforced concrete deep beams under two symmetrical point loads.

These tests revealed the following results:

1-An increase in shear capacity was observed with increasing concrete strength and decreasing shear span-depth ratio.

2-The increase in ultimate shear strength and in diagonal cracking load was attributed to the arch action for specimens with a shear span-depth ratio less than 2.5.

3-Vertical stirrup became more effective with the greater span/depth ratio.

4-Horizontal web reinforcement was more efficient in beams with shear span/depth ratio less than 1.0.

5-Web reinforcement had no effect in controlling the diagonal cracking load and cracking patterns for beam with or without web reinforcement.

Kang-Hai tan et al[14]performed experimental tests on reinforced concrete deep beams with high strength concrete under two symmetrical top loading considering two main variables; shear span-depth ratio and span-depth ratio.

The conclusions of this test are :

1-Span depth ratio has little influence in failure load for beam with $[\frac{a}{d}]>1$

2-The flexural failure became dominant with increasing span/depth ratio

3-The results of these tests insure safe design for higher strength deep beams compared with prediction based on ACI building code for concrete strength less than 41 Mpa.

Ashraf[15]carried out tests on reinforced concrete continuous deep beams considering shear-span/depth ratio, amount and type of web reinforcement and amount of main longitudinal reinforcement as main parameter of these tests.

He concluded that the vertical web reinforcement had more influence on shear capacity than horizontal web reinforcement . He also compared his results with ACI Building code and CIRIA code but it showed little agreement.

Kang-Hai Tan et al[16]reported experimental tests for reinforced concrete deep beams with cylinder compressive strength of generally exceeding 55 Mpa and main longitudinal reinforcement ratio ρ and shear span/depth ratio as main parameter of these tests .

The beams were organized into four groups with reinforcement ratio ρ=0.2 , 2.58 , 4.08 and 5.8 percent. The beams were tested for different span-depth ratio$[\frac{a}{d}]$, ranging from 0.28 to 3.14.

He concluded that :

1-The failure mode was chiefly influenced by the $[\frac{a}{d}]$ ratio and the effect of reinforcement ratio was not significant. The beam will fail in:

- Bearing mode for $[\frac{a}{d}]<0.28$
- Shear compression mode for $0.28<[\frac{a}{d}]<1.12$
- Diagonal tension mode for $1.12<[\frac{a}{d}]<2.26$
- Shear tension mode for $[\frac{a}{d}]>2.26$

2- Increasing of ρ beyond 2% did not significantly increase the shear strength of HSC deep beams. Thus this value represents a practical upper limit in maximizing the main reinforcement to augment the shear strength .

Fenwick and Paulay[4] conducted an extensive experimental investigation to study the nature , significance and parameters affecting the aggregate interlock mechanism . The parameters included in their work are concrete compressive strength σ_{co} and crack width Δ_N, which was kept constant at $0.0075 inch$. They observed that the concrete strength is a significant parameter influencing the maximum shear stress level and shear stiffness. Using regression analysis of their experimental results, shear stress is expressed as following:

$$v = (\frac{0.467}{\Delta_N} - 8.41)(0.7115\sqrt{\sigma_{CO}} - 0.409)(\Delta_S - 0.436\Delta_N) \quad \text{.....2.1}$$

Where

v=Shear stress

Δ_S = Shear displacement in inches

The shear stiffness A, of the cracked concrete is obtained by differentiating eq.(2.1) with respect to shear displacement Δ_s

$$A = \frac{\partial v}{\partial \Delta_S} = (\frac{0.467}{\Delta_N} - 8.41)(0.7115\sqrt{\sigma_{co}} - 0.409) \quad \text{.....2.2}$$

Rearranging

$$A = 0.467(\frac{1}{\Delta_N} - 18.01)(0.7115\sqrt{\sigma_{co}} - 0.409) \quad \text{.....2.3}$$

According to their results these equations are valid for crack width range from 0.0025 to 0.015 $inch$, σ_{co} in (ksi) and A in (ksi/in).

Houde and Mirza[17] in their study of shear strength of reinforced concrete beams, conducted an experimental program to establish force-displacement relation-ship at cracking due to aggregate interlock, the parameters considered are:

1-Crack width Δ_N

2-Concrete strength σ_{co}

3-Maximum aggregate size

Houd and Mirza suggested the following shear stress-displacement relation-ship:

$$v = 0.057\Delta_N^{-1.5}\Delta_S \quad \text{.....2.4}$$

$$A = \frac{\partial v}{\partial \Delta_S} = 0.057\Delta_N^{-1.5} \quad ksi/in \quad \text{.....2.5}$$

Where A, the shear stiffness, is obtained by differentiating eq.(2.4) with respect to Δ_S .

A more general equation suggested by Houde and Mirza to cover the range of crack width below Δ_N = 0.002 *inch*.

$$A = G - \frac{G^3}{\lambda\left(\frac{1}{\Delta_N}\right)^2 + G^2} \quad \text{.....2.6}$$

Where G is the elastic shear modulus of uncracked concrete and λ is a constant.

Both of the above models are valid for limited crack width and this necessitates the search for an analytical aggregate interlock model for wider range of crack widths.

In their study of the post cracking shear resistance mechanism in reinforced concrete beams with diagonal tension cracks Ngo et al[18] modeled dowel action by using the concept of effective dowel action length, which is the length over which the bond assumed to be destroyed, and they assumed an effective dowel action length to be two inches. This means using constant dowel stiffness over the entire post-cracking.

Based on experimental results Taylar suggested the following equation for peak dowel force D_f in kips:

$$D_f = 2.04 - 0.1[\sum(C_s + C_{i)}]^2\sigma_{to} \quad \text{.....2.7}$$

Where

σ_{to} = Splitting tensile strength of concrete.

C_s = Side cover to bars.

C_i = Distance between the bars.

Another expression suggested by Taylor to fit the dowel force displacement curves obtained experimentally is:

$$D = 3.48 D_f \Delta^{0.25} \quad \text{.....2.8}$$

Where

D= Dowel force (*kips*).

D_f =Cracking force (*kips*).

Δ= Dowel displacement (*inch*).

The dowel stiffness D_s may be obtained by differentiating eq.(2.8) with respect to Δ:

$$D_s = \frac{\partial D}{\partial \Delta} = 0.87 D_f \Delta^{-0.75} \quad \text{.....2.9}$$

Houde and Mirza based on experimental result suggested the following expression for Dowel cracking force D_f:

$$D_f = 0.400(\sigma_{co})^{1/3}[\sum (C_s + C_i)] \quad \text{.....2.10}$$

Also they suggested the following linear dowel force-displacement relation-ship:

$$D = 2000 D_f \Delta \quad \text{.....2.11}$$

The dowel displacement, which corresponds to the peak dowel force (cracking force)was $\Delta_c = 5 \times 10^{-4} inchs$.

The dowel stiffness D_S may be obtained by differentiating eq.(2.11) with respect to Δ:

$$D_s = \frac{\partial D}{\partial \Delta} = 2000 D_f \quad \text{.....2.12}$$

Where D_s is expressed in *kips/in*

The models viewed above have succeeded in providing useful information on the dowel mechanism but are limited to shallow beams, where the dowel failure is caused primarily by splitting along the main reinforcement.

2.2 Review of Analytical Investigation

The first attempt to use an analytical approach (finite element method) to model reinforced concrete beams up to failure was made by Ngo and Scordelis[19]. They used two dimensional constant strain triangular elements to model the concrete and steel as shown in fig 2.1(c). The bond-slip phenomenon was represented by special zero-length linkage elements connecting the plane element of concrete to those of steel at discrete points as shown in fig.2.1(b).Discrete cracking was considered in this model such that diagonal cracks were represented by separating elements on either side of the crack (by assigning two nodes, occupying the same coordinates in space, along the crack).

This investigation was not intended to explore the behavior of reinforced concrete beams in the non-linear and ultimate ranges and therefore, the materials properties were considered to be linear.

The main shortcoming of this model is:

Linearity of material.

Neglecting the effect of post-cracking shear resisting mechanism (aggregate interlock and dowel action) in shear capacity.

Absence of the effect of web reinforcement.

Difficulty to simulate bond slip mechanism due to the type of steel idealization.

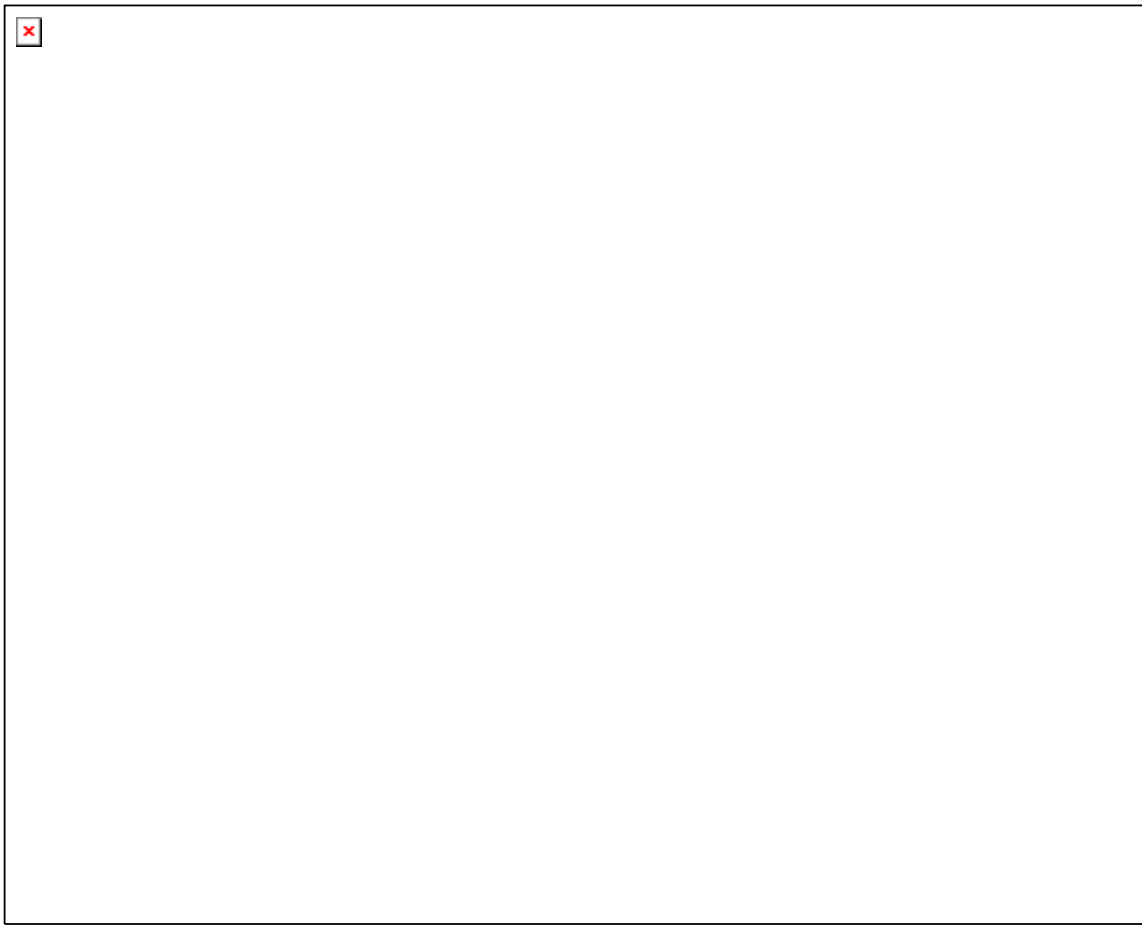

Nilson[20] extended the work of Ngo and Scordelis by adding some considerations to their model in (material properties, concrete and steel modeling and finite element technique).

Material properties were considered to be non-linear.

Concrete and steel were idealized by using improved quadrilateral plane stress finite elements.

Discrete cracking was considered in this model to model the diagonal cracking.

An incremental method is used to reload the structure after cracking.

Ngo, Franklin and Scordelis[21] introduced some refinement to this model by representing concrete and steel with quadrilateral elements and introducing the effect of stirrups, represented by one dimensional bar elements. Also they studied the post–cracking shear mechanism by using a linkage element of zero-dimension to simulate aggregate interlock mechanism and assuming that shear forces transferred by dowel action in main reinforcement can be carried by portion of this reinforcement.

The main disadvantage of this model is that non-linear behavior of reinforced concrete beam is not considered.

An important conclusion of this study is the significant contribution by dowel action and interface shear transfer to the total shear capacity of shallow beams, There is some reservation due to the existence of predefined diagonal crack from the start of loading.

Houde and Mirza studied the non-linear behavior of reinforced concrete beam and the relative contributions of shear forces transferred by aggregate interlock and dowel action to the total shear capacity but there is no account of bond-slip mechanism in their model due to the type of idealization of reinforcement.

Basic considerations of Houde and Merza model:

For material properties a non-linear uniaxial stress-strain relation was used for concrete in compression and a linear relation in tension.

Concrete was idealized by quadrilateral plane elements as well as triangular ones while the reinforcement was represented by quadrilateral elements.

Discrete cracking was considered in this model for diagonal cracking.

Franklin[22] suggested two types of finite element models:

In the first model the beam is divided into number of special type of frame elements with depth equal to the depth of the beam, These frame elements are then subdivided into ten layers, and with maximum number of reinforcement layers equal to four over this depth.

Basic considerations of the first model are:

Progressive distributed cracking was assumed to occur over frame elements.

Its ability to represent bond slip mechanism and no account is taken for the aggregate interlocking and dowel action mechanism.

This model is effective only for vertical cracks (frame element model was incapable of producing diagonal cracks).

An incremental method is used in this research to reload the beam after cracking.

In the second model materials are assumed to be non-linear and bond-slip mechanism is considered but no account is taken for the aggregate interlock and dowel action.

Basic considerations of the second model are:

Concrete is modeled as quadrilateral plane stress elements and the steel as one dimensional bar elements.

Distributed cracking in this work is used to model the diagonal cracking.

Franklin analytical models were stiffer than the actual beams.

CHAPTER (3)
MODELLING OF SHEAR MECHANISM AND POST CRACKING

There are three main mechanisms for shear transfer that can develop after cracking of reinforced concrete members:

The shear force mechanism that is transferred across cracks (aggregate interlock).

Shear force that develops in the reinforcement (dowel action).

- The stress transfer mechanism, which results in the interaction of concrete and steel (bond-slip).

3.1 Aggregate Interlock

For the aggregate interlock mechanism the surfaces of crack, which develop in concrete member, are usually irregular and rough. The occurrence of shear displacements parallel to the direction of such crack results in the transfer of shear forces by aggregate interlock from one side of crack to other side.

The main factors affecting the performance of this mechanism are:

1-Size of contact area between the surface of crack which depends primarily on crack width and shear displacement parallel to the crack .As shear displacement increases the contact area increases and as crack width decreases the contact area increases.

2-The force displacement characteristic of aggregate asperities through which the shear forces are transferred depends on:

- Compressive strength of concrete.

- Type of aggregate.

  Size of aggregate.

3.1.1 Proposed Analytical Model of Aggregate Interlock Mechanism

In this research an analytical model simulating the aggregate interlock mechanism is proposed. The primary parameters considered in this model are:

- Crack width Δ_N
- Shear displacement Δ_S
- Compressive strength σ_{C0}

The first step in constructing an analytical model must therefore be the idealization of the irregular crack surface. The possible idealization profile is shown in Fig.3.1 below

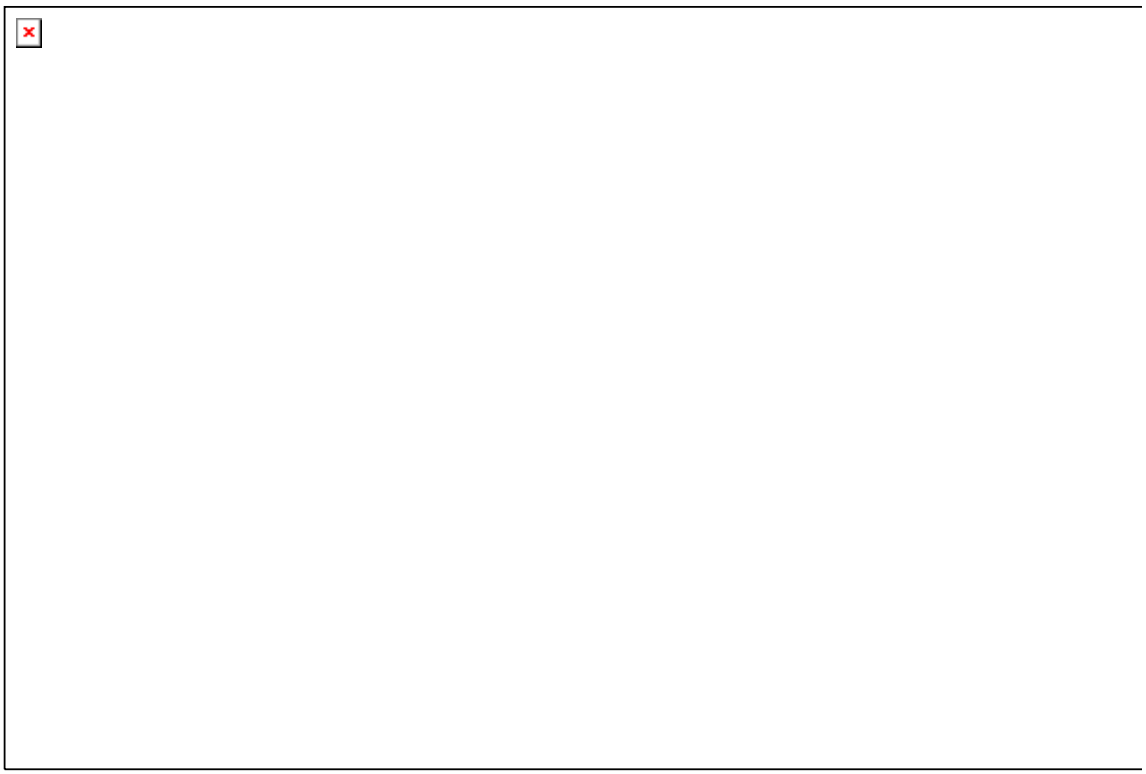

It consists of tooth like asperities having uniform geometrical properties along the entire crack. This idealization is chosen to

simplify the task of constructing an analytical model. A free-body diagram of the internal stresses acting on the idealized crack surface as shown in Fig.3.1are of two types:

- Stress normal to the crack surface
- Shear stress component tangential to the crack surface

The horizontal equilibrium condition is given by:

$V = k(\sigma_s s\cos\theta + \sigma_N s\sin\theta)$ ……3.1

Where:

σ_s = Shear stress along the crack surface.

σ_N =Stress normal to the crack surface.

s =Contact surface area for one idealized asperity.

θ =Angle between idealized crack surface and horizontal axis.

k= Number of mobilized asperities along entire crack.

The vertical equilibrium condition is given by:

$\sigma_s s\sin\theta = \sigma_N s\cos\theta$ ……3.2

or

$\sigma_N = \sigma_s \tan\theta$ ……3.3

By substituting eq.(3.3) in eq.(3.1)

$V = ks\sec\theta\sigma_s$ ……3.4

In this research the non-linear relationship below is suggested(as that of Nilson).

$\sigma_S = R_1\xi^m$ ……3.5

where:

σ_S = Amount of slip along inclined crack surface.

R_1, m = Parameters to be obtained from experimental data.

ks = Total contact area along the entire surface of crack.

From Fig.3.2.

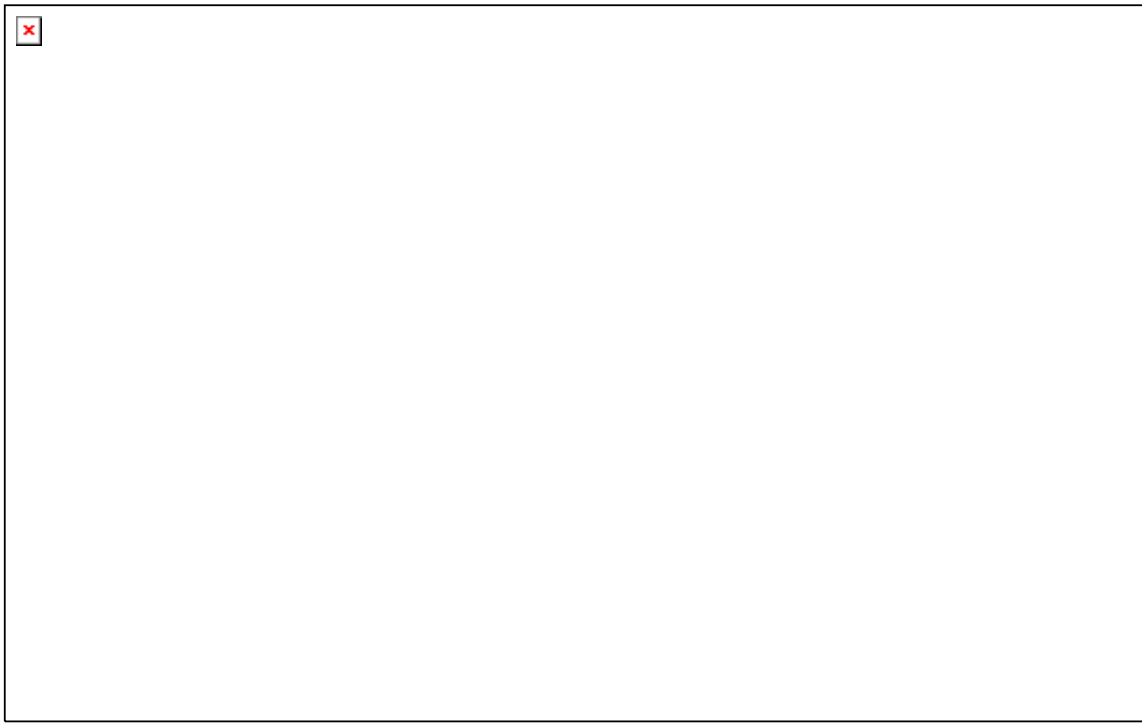

$$\xi = (\Delta_S^2 + \Delta_N^2)^{1/2} \quad \text{.....3.6}$$

where :

Δ_S =Shear displacement.

Δ_N =Crack width.

A linear relation is assumed to exist between ks and Δ_S :

$$ks = R_2 \Delta_S \quad \text{.....3.7}$$

where

Δ_s, R_2= Parameters to be obtained from experimental data.

By substituting eq.(3.5)and eq.(3.7) in eq.(3.4)

$$v = C(\Delta_S^2 + \Delta_N^2)^n \Delta_S \quad \text{.....3.8}$$

Where:

$$C = \frac{R_1 R_2 \sec\theta}{A_{Shear}} \quad \ldots\ldots\ldots\ldots\ldots\ldots\ldots\ldots\ldots\ldots\ldots\ldots\ldots\ldots\ldots\ldots\ldots\ldots 3.9$$

and n=0.5

The shear stiffness A of cracked concrete is obtained by differentiating eq.(3.8) with respect to Δ_S:

$$A = \frac{\partial v}{\partial \Delta_S} = C([1+2n]\Delta_S^2 + \Delta_N^2)(\Delta_S^2 + \Delta_N^2)^{n-1} \quad \ldots\ldots\ldots\ldots\ldots\ldots\ldots\ldots\ldots 3.10$$

eq.(3.8) and eq.(3.10) express the shear stress and shear stiffness as non-linear function of the crack width Δ_N and shear displacement Δ_s. The only unknown parameters in this equation are C and n, which can be obtained from experimental work.

The experimental data used in this research are these parameters adopted by Fenwick and paulay.

The main parameters of their experimental work are:

1-Crack width.

2-Compressive strength.

Firstly concrete strength is assumed to be constant with value 4.81 *ksi* and the crack width varies between (0.0025-0.015*inch*). The relation between v_u and Δ_N can be obtained from Fig.3.3.

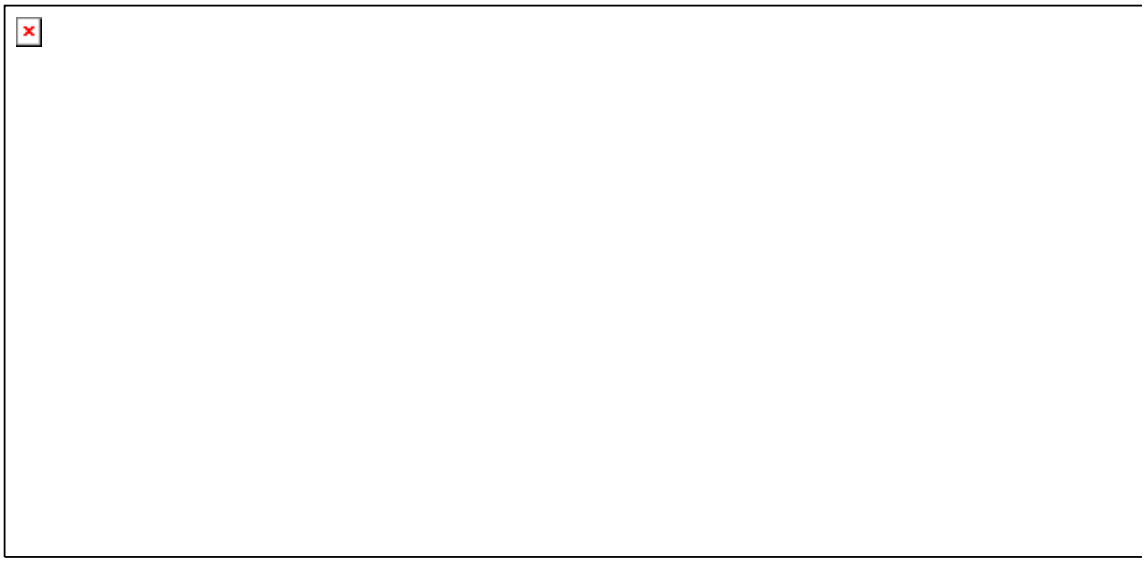

Where

v_u = Shear stress at failure.

$v_u = C_1(0.3 - 10.42\Delta_N)\ for \sigma_{co} = 4.81 ksi$ ……3.11

Secondly crack width is assumed to be constant with a value of 0.0075inch. The relation-ship between v_u and compressive strength σ_{C0} can be obtained from Fig.3.4.

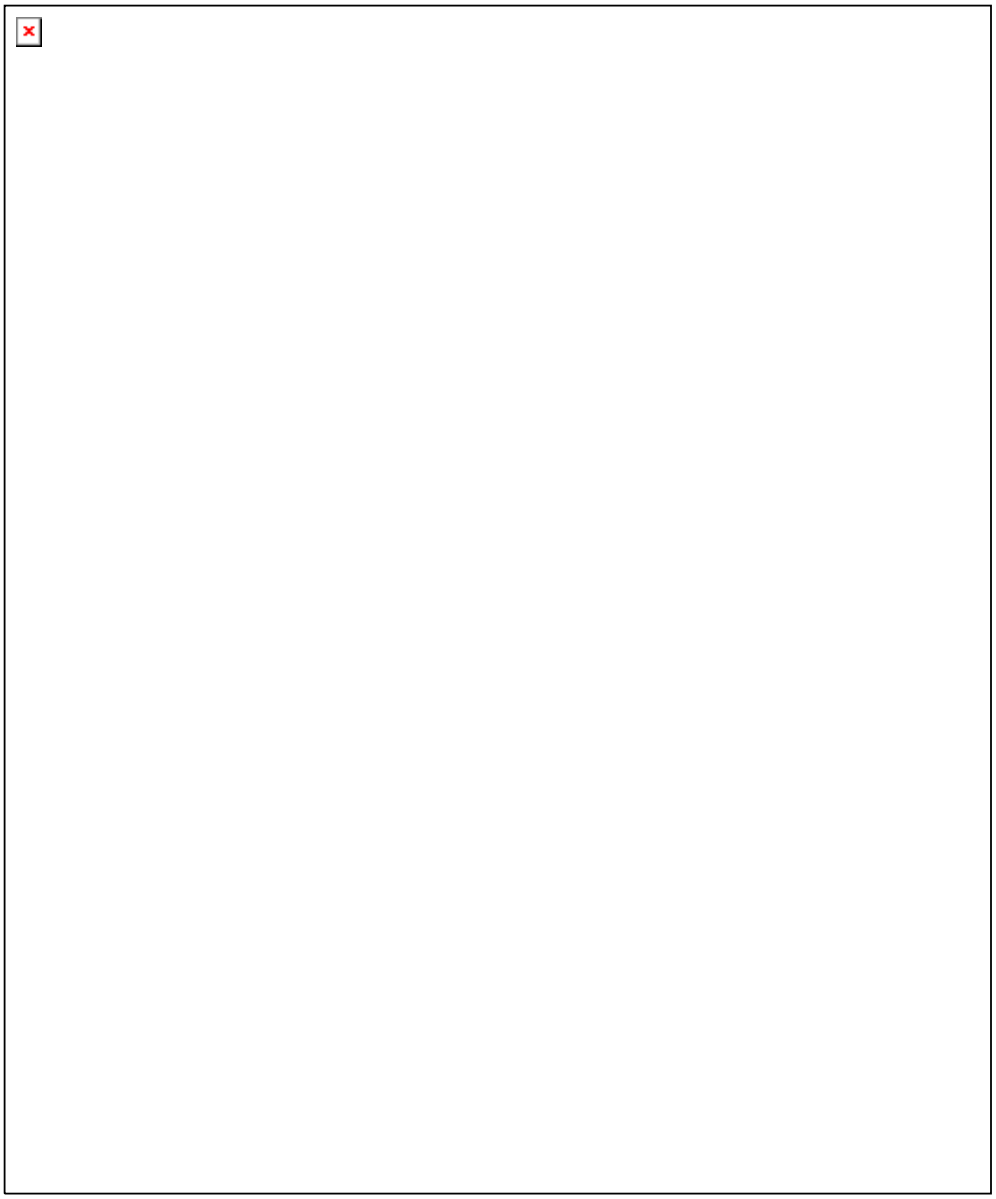

This relation can be expressed by

$$v_u = 0.0576 + 0.031\sigma_{co},\ for \Delta_N = 0.0075 inch \quad \ldots\ldots\ldots\ldots\ldots\ldots\ldots\ldots\ldots\ldots 3.12$$

We can find parameter C_1 by substituting maximum shear stress v_u corresponding and Δ_N=0.0075 inch the following equation

$$C_1 = v_u / (0.3 - 10.42\Delta_N) \quad \ldots\ldots\ldots\ldots\ldots\ldots\ldots\ldots\ldots\ldots\ldots\ldots\ldots\ldots\ldots\ldots 3.13$$

Which gives $C_1 = v_u / 0.22 \quad \ldots\ldots\ldots\ldots\ldots\ldots\ldots\ldots\ldots\ldots\ldots\ldots\ldots\ldots\ldots\ldots 3.14$

By substituting eq (3.12) in eq.(3.14)

$$C_1 = 0.262 + 0.1413\sigma_{co} \quad \ldots\ldots\ldots\ldots\ldots\ldots\ldots\ldots\ldots\ldots\ldots\ldots\ldots\ldots\ldots\ldots\ldots\ldots\ldots\ldots 3.15$$

This equation is plotted in Fig.3.5 and the values of parameter C_1 based on shear stress-displacement curves corresponding to Δ_N= 0.0075*inch*. This equation can be applied to other crack widths.

The relation between the shear displacements Δ_{su} corresponding to maximum shear stress v_u can be obtained from Fig.3.6 corresponding to crack width between (0.0025-0.015 *inch*) using method of least-square. This relation can be written as follow:

$$\Delta_{su} = 7.517 * 10^{-4} + 0.638\Delta_N \quad \ldots\ldots\ldots\ldots\ldots\ldots\ldots\ldots\ldots\ldots\ldots\ldots\ldots\ldots\ldots\ldots\ldots\ldots\ldots\ldots 3.16$$

By considering boundary conditions of shear stress-displacement curves given in Fig.3.7 in conjunction with equations above the unknown parameters *C* and *n* can be obtained as follows:

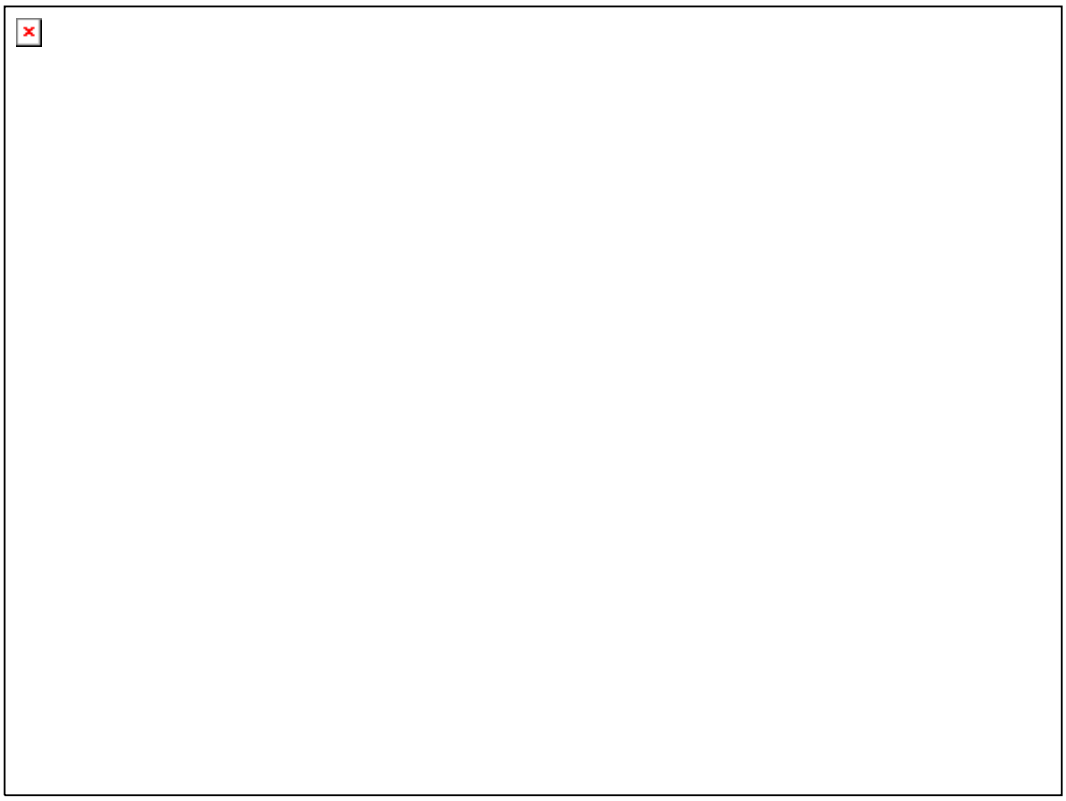

a / $\Delta_S = \Delta_{su}$ when $v = v_u$

Substituting the expression above in eq.(3.8)

$$v_u = C(\Delta_{su}^{\ 2} + \Delta_N^{\ 2})^{-n}\Delta_{su} \Rightarrow \quad C = \frac{v_u}{\Delta_{su}}(\Delta_{su}^{\ 2} + \Delta_N^{\ 2})^{-n} \qquad \text{.....3.17}$$

b/ at inception of loading

$S = 0$, $A = A_0$ for $N = N_0$

Substituting the expression above in eq.(3.17)

$$C = A_0(\Delta_{N_0})^{-2n} \qquad \text{.....3.18}$$

Equating eq.(3.17) and eq.(3.18)

$$n = \frac{\ln\left(\frac{v_u}{A_0 \Delta_{su}}\right)}{\ln\left(\frac{\Delta^2_{su} + \Delta^2_N}{\Delta^2_N}\right)} \quad \text{.....3.19}$$

The value of v and A can be obtained by the following procedure:

1/Calculate C_1 from eq.(3.15).

2/Calculate v_u by substituting C_1 in eq.(3.11).

3/Calculate Δ_{su} from eq.(3.16).

4/Calculate n by substituting v_u and Δ_{su} in eq.(3.19).

5/Calculate C by substituting n in eq.(3.18).

Then obtained the value of v and A by substituting n and C in eq.(3.8) and eq.(3.10) respectively.

This approach of aggregate interlock modeling is used in connection with discrete cracking. Linkage elements are used to lock or release the node pairs defined along discrete crack .The two orthogonal fictitious springs stiffness k_h and k_v are assigned values when cracking is detected in elements adjacent to the node-pairs,

$k_h = a_s A$

$k_v = 0$

Where

a_s = cracked surface area corresponding to a linkage element .

This modeling can not be used in connection with distributed cracking because of difficulty of obtaining Δ_N and Δ_s due to the assumption of displacement continuity across crack in this approach, and eq.(3.10) can not be applied to determine shear stiffness.

To solve this problem many investigators use the concept of reduced shear modulus G. This concept may be explained as

follow: when cracking occurs, the shear term is reduced by a certain factor to account for capacity of cracked concrete to carry shear by aggregate interlock.

The choice of this factor was determined by trying several reduction factors and selecting the factor, which gives prediction closet to experimental results. In this research a proposal for an expression for *G* suggested by Nilson is selected .The main concept of this proposal can be explained as follow:

Tensile strain normal to crack ε_1 may be used to define the reduced shear modulus *G*.

The change of *G* with ε_1 should be rapid and non-linear.

At failure of member the value of *G* becomes very small (this is to reflect the fact that at failure, the cracks become too wide to be able to transfer a significant amount of shear stresses).

The following relation between G-ε_1 is suggested by Nilson:

$$G = G_1 \; for \varepsilon_1 < \varepsilon_{t0} \quad \text{.....3.20}$$

$$G = 0.4G_1 / \frac{\varepsilon_1}{\varepsilon_{t0}} \; for \varepsilon_1 \geq \varepsilon_{t0} \quad \text{.....3.21}$$

Where

ε_{t0} = Cracking tensile strain.

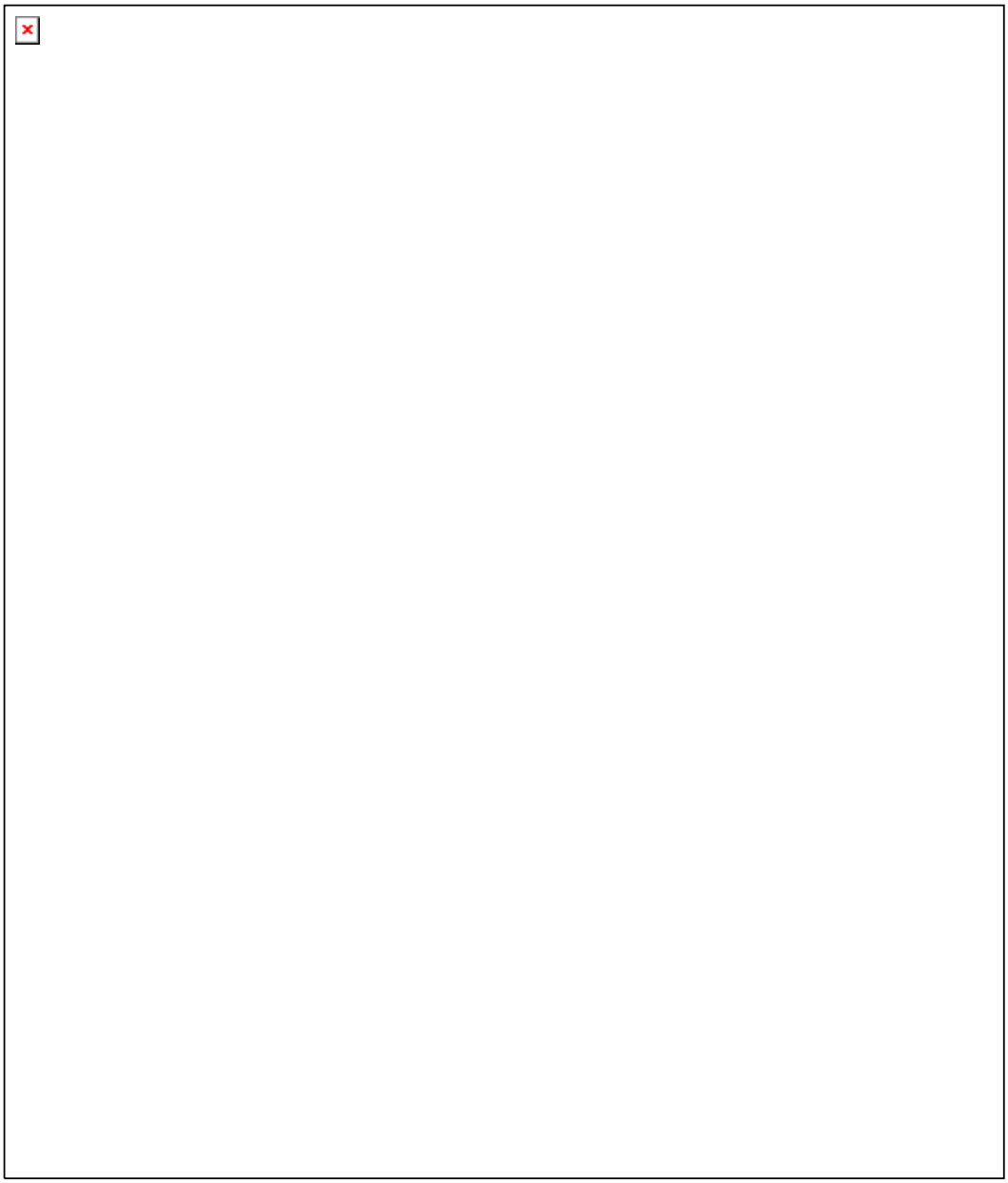

This relation assumes that at inception of cracking (when $\varepsilon_1 = \varepsilon_{t0}$) the shear modulus G is reduced to 40% of shear modulus of uncracked concrete G by substituting the value of ε_1 in eq.(3.20).

When ε_1 is increase and reaches the value ($\varepsilon_1 = 5\varepsilon_{t0}$) at failure the shear modulus reduces to 0.08 *G* by substituting the value of in eq.(3.21)

The main function of this model was to reach a reliable estimate of the contribution of aggregate interlock to total shear resistance in beams.

Factors affecting this mechanism are:

a- Concrete compressive strength.

b- Crack width.

The post-cracking shear resistance mechanism to aggregate interlock has attracted considerable research effort in recent years. In this regard, the finite element method has played a prominent role.

The mode of representation of aggregate interlock mechanism in finite element model depends on the type of crack and type of model used. Across discrete crack, special linkage elements with orthogonal fictitious spring are used. A nonlinear stiffness characterization for such springs is derived from an analytical model in conjunction with experimental data. In cases where distributed cracking is employed, a reduced shear stiffness G is employed in the constitutive relation of cracked concrete. A non-linear expression relating *G* to the tensile strain normal to the crack direction is proposed.

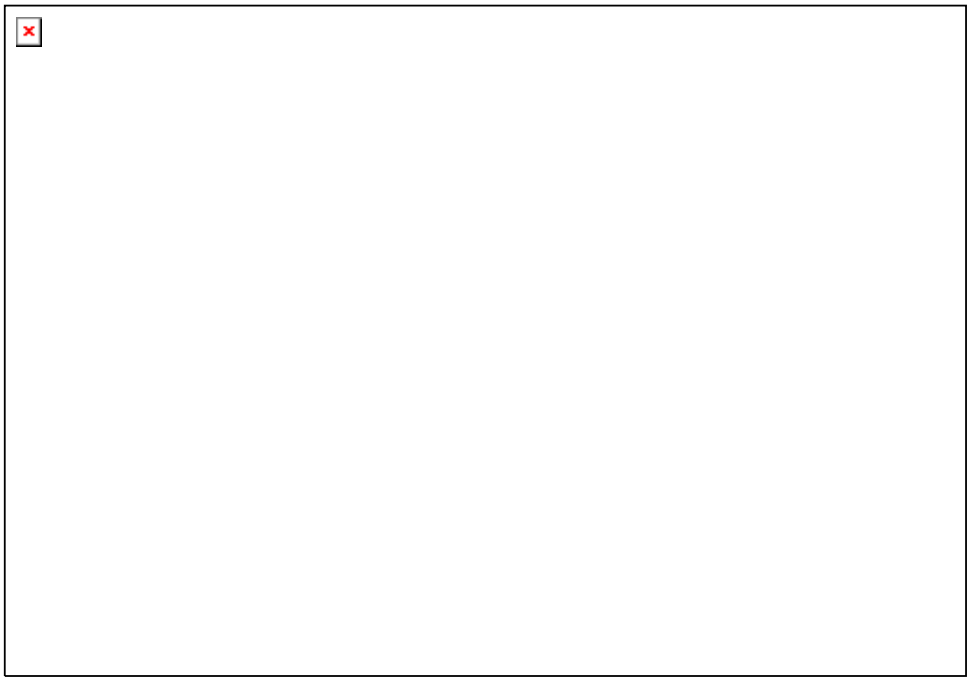

3.2Dowel Action Mechanism

The reinforcement provided to carry tensile forces along its axis can also resists forces normal to its axis. This occurs when such reinforcement crosses sufficiently open crack. This additional resistance is known as dowel action mechanism.

There are many factors affecting this mechanism:

a- Reinforcement ratio A_s/bd.

b- Reinforcement bar diameter.

c- Yield strength of reinforcement bar $f_{y.}$

d - Angle between the bar and the normal to the crack surface.

e- Concrete compressive strength f_{cu}.

f- Shear span.

3.2.1 Proposed Analytical Model of Dowel Action Mechanism

In this research an analytical model similar to that of Nilson is used. This model is based on experimental results of Dulacska which simulate dowel action mechanism as follows:

A dowel bar is embedded in concrete and can be treated as a semi-infinite beam on elastic foundation as shown in Fig. 3.10.

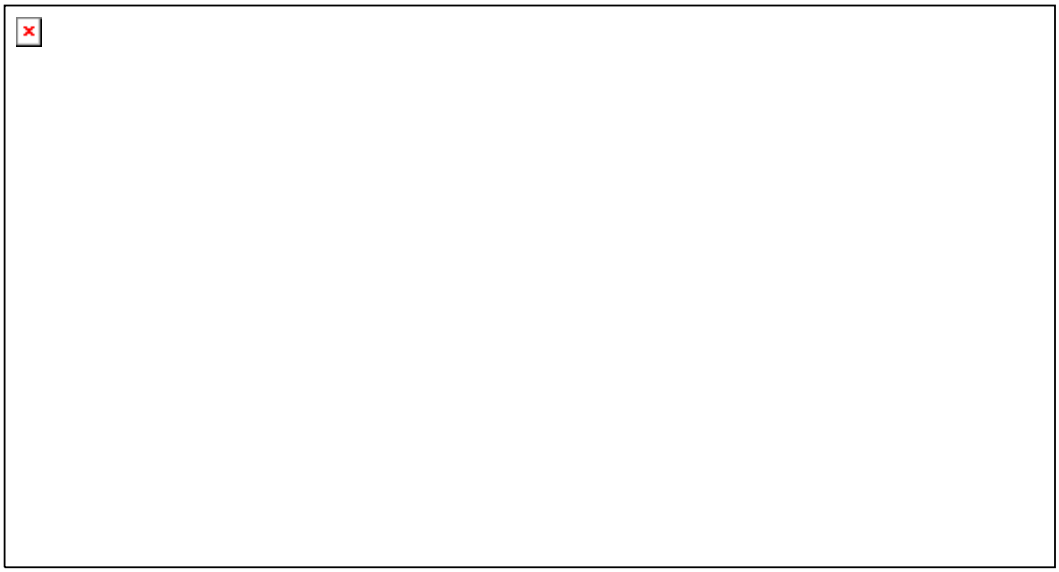

The bar is assumed to be fixed freely over crushed portion of concrete. The dimension *C* defines the extent of this crushing and is expressed as follows:

$$C = \gamma \frac{\sigma_y}{\sigma_{co}} \phi \sin\delta \quad \ldots\ldots\ldots\ldots\ldots\ldots\ldots\ldots\ldots\ldots\ldots\ldots\ldots\ldots\ldots\ldots\ldots\ldots\ldots\ldots 3.22$$

Where *C* and ϕ are expressed in inches and σ_y and σ_{co} in *ksi* and γ is a dimensionless constant to be obtained from experimental data. This expression is based on the following assumptions:

1/ The higher concrete strength the lower amount of crushing *C*.

2/ The amount of crushing *C* increases as quantity $\phi\sigma_y$ (which reflect the bar rigidity) increases.

3/ Direct dependency is assumed to exit between *C* and angle of inclination δ expressed in the form $sin\delta$. The implication of this is that no crushing occurs when $\delta=0$,when the bar is perpendicular to the shear plane, and that as δ increases the dimension *C* increases.

The stress distribution beneath the dowel bar is shown in Fig.3.11. It is governed by following expression:

$$q = D\frac{\pi}{t} e^{\frac{-\pi x}{2t}} \cos\frac{\pi x}{2t} \quad \ldots\ldots\ldots\ldots\ldots\ldots\ldots\ldots\ldots\ldots\ldots\ldots\ldots\ldots\ldots\ldots\ldots\ldots\ldots\ldots 3.23$$

Where

D = Dowel force applied at the shear plane.

t = Distance along the bar defined in Fig.3.11.

it is possible to replace the actual stress distribution in Fig.3.11(b) by simpler one using equivalent rectangular stress blocks as shown in Fig.3.11(c) the stress intensity can be obtain from the following expression:

$$q_e = \frac{1}{t}\int_0^t q\,dx \quad \text{......} 3.24$$

for $x=0$ *to* t

by substituting eq.3.23 into eq.3.24

$$q_e = \frac{1}{t}\int_0^t D\frac{\pi}{t}e^{\frac{-\pi x}{2t}}\cos\frac{\pi x}{2t}dx = \frac{1.208D}{t}(k/in.) \quad \text{.....3.25}$$

for $x=t$ *to* $3t$

$$q_e = \frac{1}{2t}\int_t^{3t} D\frac{\pi}{t}e^{\frac{-\pi x}{2t}}\cos\frac{\pi x}{2t}dx = \frac{-0.217d}{2t}(k/in.) \quad \text{.....3.26}$$

for $x=3t$ *to* $5t$

$$q_e = \frac{0.009D}{2t}(k/in.) \quad \text{.....3.27}$$

(This value is very small compared with other values; therefore stresses in region $x \geq 3t$ may be neglected). In this modeling Dulascka neglected all the stresses in the region $x \geq t$ and considered the stress block in region $x \leq t$

$$M = D * x - q_e \frac{x^2}{2} \quad \text{.....3.28}$$

Maximum bending moment occurs at a point where the shear $(V=dM/dx)=0$.

$$V = D - q_e * x = D - (1.208\frac{D}{t})x = 0 \quad \text{.....3.29}$$

Which gives $x = 0.82t$

The distribution of radial stresses along the circumference of the dowel bar is shown in Fig3.11. This distribution is governed by the following equation:

$$\sigma_r = \sigma_0 \cos\theta \quad \text{.....3.30}$$

Where

θ = Angle defined in Fig.3.10.

σ_0 = Radial stress at angle ϕ, in *ksi*

σ_r = Max. radial stress which occurs at $\theta = 0$, in *ksi*

$$q_e = 2\int_0^{\frac{\pi}{2}} \sigma_r \frac{\phi}{2} \cos\theta d\theta \quad \text{.....3.31}$$

$$\frac{1.208D}{t} = \sigma_0 \phi \int_0^{\frac{\pi}{2}} \cos^2\theta d\theta \quad \text{.....3.32}$$

where

$$t = 0.650 \frac{D}{\phi \sigma_0} \quad \text{.....3.33}$$

ACI Code specifies that σ_p should not exceed $1.445\sigma_{to}$, and eq.(3.33) becomes

$$t = 0.5 \frac{D_f}{\phi \sigma_{c0}} \quad \text{.....3.34}$$

where

D_f = The dowel force at failure.

Max. external moment can be obtain by calculating the area under curve in Fig.3.11

M= area of rectangular + area of triangular

$$M = C * D_f + 0.82t * \frac{D_f}{2} = D_f \ (C + 0.41t) \quad \text{.....3.35}$$

This moment is resisted internally by plastic yield moment M_{Py}

$$M_{py} = \frac{1}{6}\phi^3 \sigma_y = Z_p \sigma_y \quad \text{.....3.36}$$

where

Z_p = Plastic modulus of section

Equating eq.(3.35) to eq.(3.36) gives

$$D_f (c + 0.41t) = \frac{1}{6}\phi^3 \sigma_y \quad \text{.....3.37}$$

Substituting the values of *C*, *t* given by eq.(3.22) and eq.(3.34) respectively in eq.(3.37) the following quadratic equation can be obtained

$$0.205 {D_f}^2 + (\gamma \sigma_y \phi^2 \sin\delta) D_f - 0.167 \phi^3 \sigma_y \sigma_{c0} = 0 \quad \text{.....3.38}$$

Dulascka[3] estimated the parameter γ to be equal to 0.05.

The solution of eq.(3.38) is:

$$D_f = 0.13\sigma_y \phi^2 \sin\delta[\sqrt{1+\frac{54.67\sigma_{co}}{\sigma_y \sin^2\delta}} - 1] \quad \text{.....3.39}$$

For $\delta=0$, and

$$D_f = 0.92\phi^2\sqrt{\sigma_y \sigma_{co}} \quad \text{.....3.40}$$

The dowel force–displacement relation is:

$$\Delta = \frac{3D}{10^3 \phi}[\frac{1}{\sigma_{C0}}\tan(\frac{D}{D_f}\frac{\pi}{2})]^{0.5} \quad \text{.....3.41}$$

Several determinate forms of *D-Δ* relations may be used to fit the experimental response of *D-Δ*. In this research the following polynomial is suggested:

$$D = (C_1 + C_2\Delta^m)\Delta \quad \text{.....3.42}$$

Where C_1, C_2 and m are parameters to be obtained from experimental data .The dowel stiffness D_s may be obtained by differentiating the above expression with respect to Δ:

$$D_S = \frac{\partial D}{\partial \Delta} = C_1 + C_2(m+1)\Delta^m \quad \text{.....3.43}$$

By considering the boundary condition of a typical dowel force-displacement obtain experimentally, the following can be noticed:

1/ at the initiation $D_S = D_{S0}$ when $\Delta = 0$

2/ when the dowel force reaches the maximum value D_f the dowel displacement reaches a value $\Delta = \Delta_f$

3/ when dowel force exceeds D_f the *D-Δ* becomes flat, the dowel stiffness D_S reduces to zero:

By substituting these three condition in eq.(3.42) and eq.(3.43) the values of C_1 ,C_2 *and* m can be obtained as follows:

$C_1 = D_{S0}$

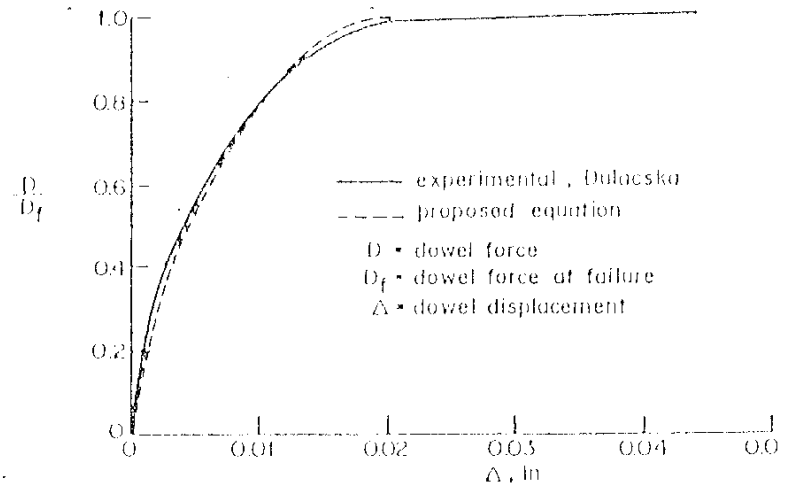

Fig.3.12 Dowel Force-Displacement Curves

$$m = \frac{1}{\frac{D_{S0}}{D_{Sf}} - 1}$$

Where

D_{sf} = Secant dowel stiffness at failure.

$$D_{sf} = \frac{D_f}{\Delta_f} \quad \text{.....3.44}$$

$D_{s0} = 667 k/in.$

The initial dowel stiffness D_{s0} may be estimated to be 667 k/in

C_1 = 667

C_2 = 1208

m = 0.198

$$D = (667 - 1208\Delta^{0.198})\Delta \quad \text{.....3.45}$$

This expression is plotted in Fig.3.12 and gives good results compared with several experimental curves done by Dulacska.

Linkage elements similar to those used in connection with aggregate interlock mechanism are employed to model the dowel

action mechanism. Upon the formation of discrete crack, a dowel stiffness D_s defined by equation is assigned to the fictitious spring parallel to crack

$$K_h = D_s$$

$$K_v = 0$$

Thus it can be concluded that the stiffness of the dowel action can be calculated from eq.(3.43) .

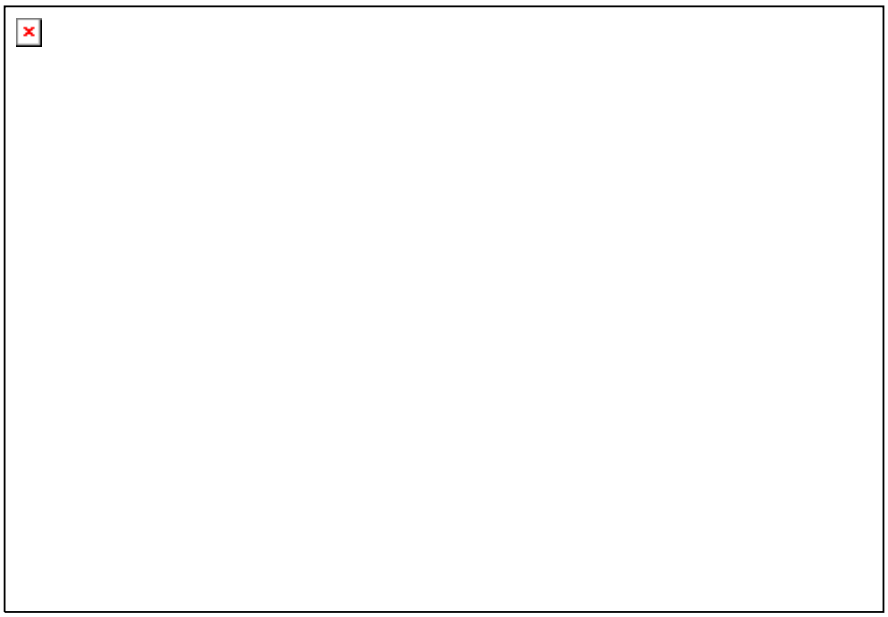

3.3 Bond Slip Mechanism:

The interaction between the reinforcement and concrete in reinforced concrete structures occurs by means of shear transfer mechanism known as bond. This bond between the steel and concrete at the interface does not remain intact, resulting in relative movement (slip) between the two components.

The importance of including such a bond-slip mechanism in a finite element model is due to its direct influence on the width and spacing of tensile cracks as well as the distribution of stress in partially cracked concrete.

Factors affecting this mechanism:

1- Compressive strength of concrete $\sigma_{co.}$

2- Peak bond stress *(ksi)*.

3-Distance from the end of specimen to the face of crack C as shown in Fig.3.14.

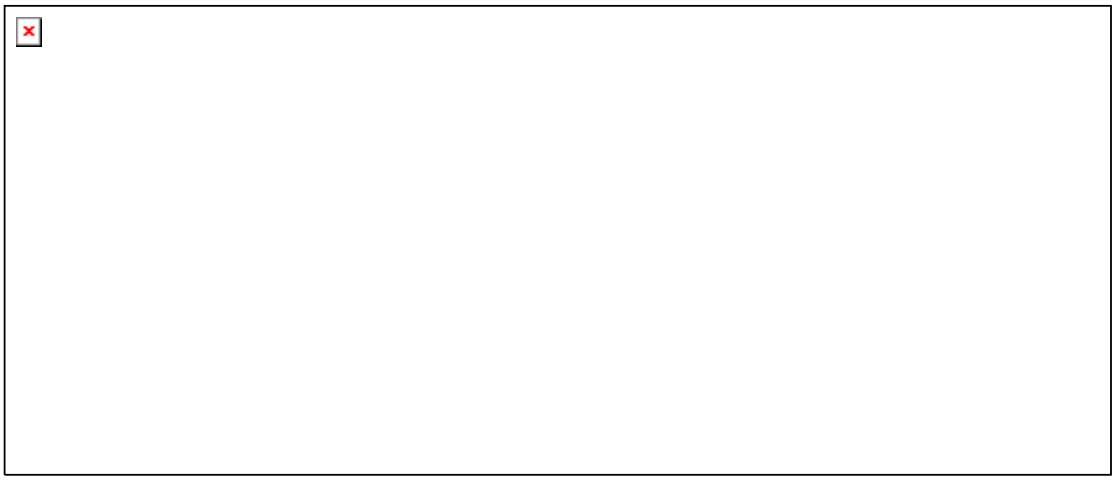

3.3.1 Proposed Analytical Model of Bond-slip Mechanism

The transfer of stress by bond between concrete and steel is most difficult to model realistically. In this research an analytical model simulating the bond slip mechanism proposed by Nilson is used. Closely spaced spring linkages are used. Each linkage contain two springs, one acting parallel to the bar axis and the other acting perpendicular to it as shown in Fig.3.15, Every short

segment of the bar is directly joined to the adjacent bar segments, and is connected to the adjacent concrete by the linkage springs. The dimension of each spring may be reduced to zero (dimensions less linkage). In the practical cases, it is usually convenient to specify one such linkage at the top of a bar segments, and one at the bottom, considering bond in its usual sense, only longitudinal spring needs to be included.

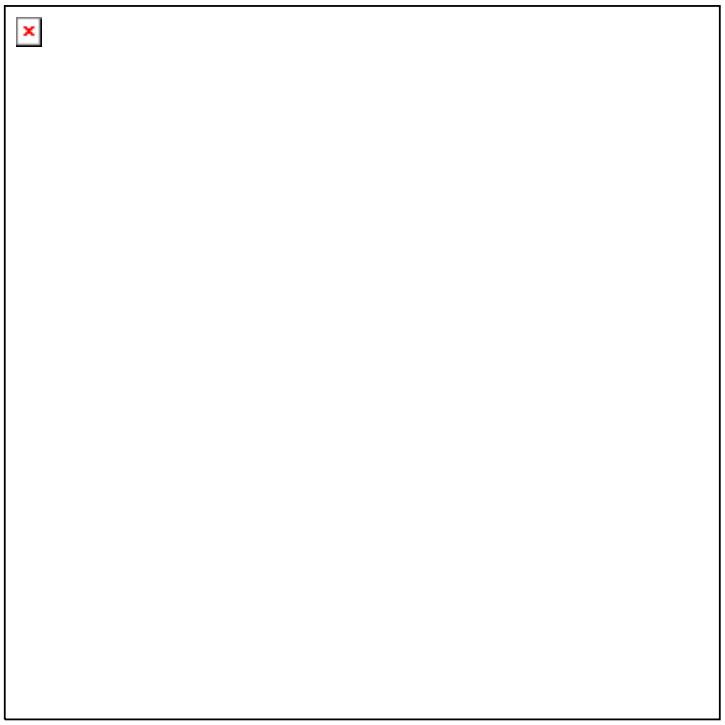

Basic assumptions of this model:

Non linear materials properties

Non homogeneity

Non linear bond slip relations

Local bond destruction

Local slip must be obtained indirectly. It is defined as the difference between steel displacement and concrete displacement in the direction of the bar axis at any section. Steel displacement is found from measured strains, while concrete displacement is

estimated from experimental work by measuring slip at the face of the tested specimens.

In this work a bond slip equation is derived indirectly from experiments reported by Bresler and Bertero[24]. Nilson has conducted such an experimental program and obtained information of direct relevance to finite element model. Nilson found that the peak bond stress U_p is proportional to the distance from the end of the specimen C (or the face of crack) as shown in Fig.3.14. This relation was presented by:

$$\frac{U_p}{\sqrt{\sigma_{C0}}} = 0.0316(1.43C + 1.5) \quad \text{.....3.46}$$

A bond stress–curve for C=6in established by Nilson and the same curve for different value of C obtained by Houde and Mirza is plotted in Fig.3.16

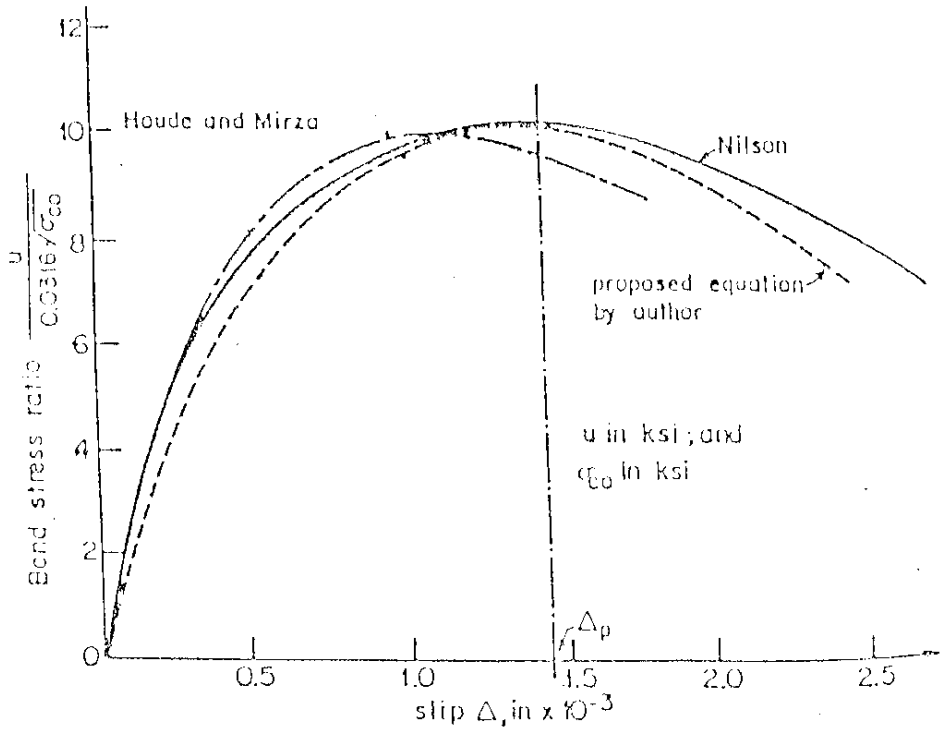

Fig.3.16 Bond stress-slip relationship

But for purpose of simplicity, the influence of *C* be may neglected and the bond stress-slip curve of Nilson with *C*= 6inch is used and the two following relations are obtained:

$$\frac{U}{\sqrt{\sigma_{c0}}} = 0.0316(7.5\alpha^3 - 25\alpha^2 + 27.5\alpha) \; for 0 \le \alpha < 1 \quad \ldots\ldots\ldots\ldots\ldots\ldots\ldots 3.47$$

$$\frac{U}{\sqrt{\sigma_{c0}}} = 0.0316(25\alpha^3 + 15\alpha^2 + 22.5\alpha) \; for \alpha \ge 1 \quad \ldots\ldots\ldots\ldots\ldots\ldots\ldots 3.48$$

U = bond stress, *ksi*

$$\alpha = \frac{\Delta}{\Delta_P} \quad \ldots\ldots\ldots\ldots\ldots\ldots\ldots 3.49$$

where

α=Normalized slip

Δ=Slip, inch.

$\Delta_{p=}$ Slip at peak bond stress, inch.

The dotted line in Fig3.16 is a plot of these two polynomials and is very close to experimental curve. To establish the non linear bond stiffness Eq.(3.47) is differentiated with respect to α

$$B_s = \frac{\partial U}{\partial \Delta} = 0.0316 \frac{\sqrt{\sigma_{c0}}}{\Delta_P}(22.5\alpha^2 + 50\alpha + 27.5) \quad \ldots\ldots\ldots\ldots\ldots\ldots 3.50$$

equivalent spring linkage stiffness can be obtained by multiplying the above expression by the surface area tributary to one linkage to obtain stiffness in proper units.

$$K_h = B_s A_s \quad \ldots\ldots\ldots\ldots\ldots\ldots\ldots 3.51$$

Where

A_s = surface area of reinforcement bar

In this modeling it is assumed no appreciable relative displacement normal to the bar occurs. Therefore stiffness value $K_v = 10K_h$ is used in this research to impose this condition.

CHAPTER(4)

FINITE ELEMENT MODELING

4.1 Basic Concepts

The finite element method is a numerical technique for obtaining approximate solution to variety of engineering problems. During the last fifty years many problems in aeronautical, civil, mechanical and nuclear engineering, which required the determination of static as well as dynamic response, have been solved by the finite element method.

The basic concept in the finite element method is to find the solution of a complicated problem by replacing it by a simpler one. This is done by modeling analytically a continuous structure and subdividing it into regions or elements. Each element is described by a separate functional representation. These subdivisions considered to be interconnected at specified joints, which are called nodes or nodal points usually lying on the element boundaries where adjacent elements considered to be connected. In totality, these subdivisions follow the behavior of the real continuous structure with a certain marginal error inherent in the method itself, like any other numerical method. The amount of such an error depends primarily on the functional representation (modeling) chosen to best resemble the continuous behavior of actual structure, and upon the size of element relative to the size of the region studied.

The application of the finite element method to non-linear problems results in more numerical operations compared to linear problems. However, recent developments of the digital computers overcome this point.

Since the finite method uses a substitute structure whose parts are, in a sense, pieces of actual structure, solutions of complicated problems are expected to be approximate .In most complicated problems approximate solutions are acceptable as the

exact solutions are too elaborate or rather impossible to obtain. The non-linear problems must satisfy the fundamental conditions of equilibrium, compatibility and constitutive relations of material. The non-linear solution is obtained by solving a series of linear problems such that at the final stage appropriate non-linear condition are satisfied.

4.2 Non-linear Analysis

Non-linearity which occur in structures are of two types:

- Geometric non-linearity
- Material non-linearity

The first is caused by large displacements in the structure, the second results from non-linearity in materials (stress-strain relationship). The geometric non–linearity is of very little importance in reinforced concrete structures because the displacements in such structures are generally small. In this research this type of non-linearity is neglected and only the effects of material non-linearity are considered.

The main sources of material non-linearity in reinforced concrete structures are:

- Cracking of concrete
- Yielding of reinforcement
- Non-linear stress-strain relation for concrete
- Concrete-reinforcement interaction (bond-slip), and interface shear transfer due to aggregate interlocking and dowel action.

4.3 Non-linear Numerical Techniques using Finite Element Method

The solution of non-linear problems by the finite element method is usually attempted by one of three basic techniques:

1- Incremental, or stepwise procedures
2- Iterative or Newton methods
3- Step-iterative or mixed procedures

The basis of incremental procedure is the division of load into many small increments, which are not necessarily equal. During the application of each load increment, the stiffness matrix is assumed to be fixed, linear relation between load and displacement is assumed. The displacement resulting from load increments are accumulated to give the total displacement at stage of loading. This process is repeated until the total load is reached. Using small increments improve the accuracy of the method but results in more computational effort.

In the iterative procedure the full load is applied to the structure and the internal stresses are computed. A load system equivalent to the computed stresses is evaluated and checked against the applied loading system. Since an approximate stiffness matrix is used, residual forces result due the lack of equilibrium. These residual forces are then applied to the structure to restore equilibrium and additional displacements are computed. The process is repeated until the residuals are sufficiently small.

The mixed procedure utilizes a combination of the incremental and iterative schemes. The load is applied incrementally, but after each load increment successive iterations are performed until equilibrium is achieved to an acceptable level of accuracy. This procedure tends to minimize the disadvantages of previous

two methods and yields higher accuracy but needs more computational effort.

The non-linear numerical method used in this investigation can be identified as combined incremental-constant stiffness iterative method (mixed procedure).
It is evident from the procedure outlined above that the global stiffness matrix is updated only at the beginning of each load increment and maintained unaltered throughout the iterative process. The other alternative is to update the stiffness matrix after each iteration but need more computational effort.

4.4 Selection of Element and Representation of Cracking

The choice of the type of elements to idealize a certain structure depends not only on its load-carrying characteristics, but also in its geometry, degree of accuracy and admissibility conditions.
The primary features of structures to be studied in this research are:

- Composite nature of reinforced concrete.
- The interaction between the reinforcement and concrete (bond slip).
- The shear resistance mechanism, which develops after cracking (Aggregate interlock + dowel action).

A proper representation of these characteristics requires the employment of three types of elements:
1- Plane elements to represent concrete.
2- Line elements to represent the reinforcement.
3-Linkage elements to represent the reinforcement-concrete interaction and post cracking shear mechanism.

4.5 Modeling of Steel Reinforcement

In developing a finite element method of a reinforced concrete member, one of the following three alternative representations of reinforcement may be used:

1- Distributed

2- discrete

3- embedded

In the case of a distributed representation, the steel assumed to be distributed over the concrete elements, with particular orientation angle θ. Perfect bond between steel and concrete is assumed so that a composite concrete-reinforcement constitutive relation can be derived. Distributed representation, though easy to implement, is very unrealistic as the reinforcing bars are no longer uniaxial members embedded inside the concrete and bonded to it.

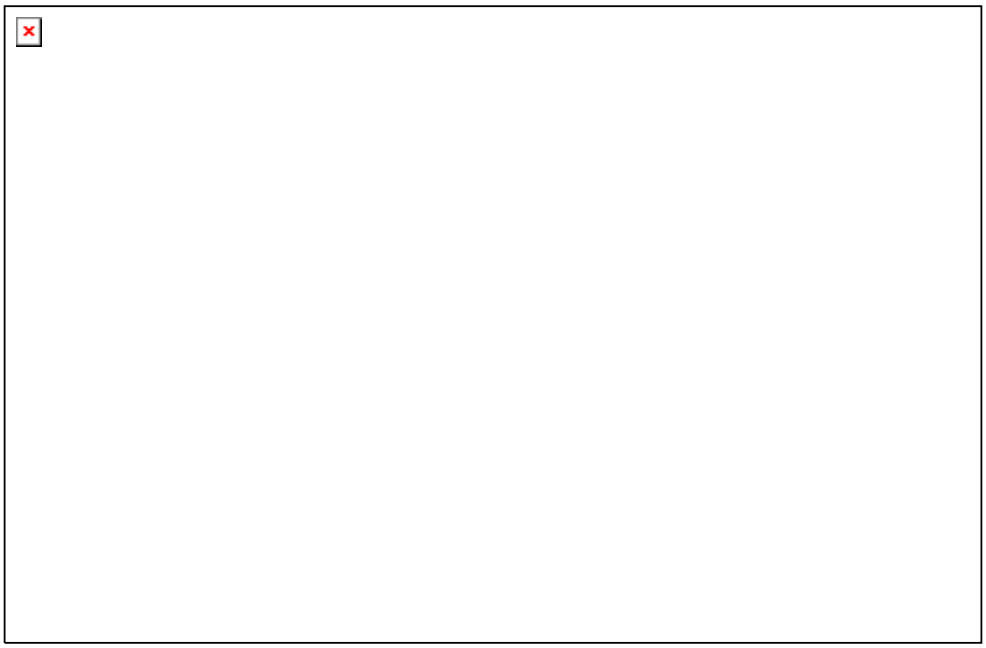

A discrete representation of reinforcement, using one-dimensional elements has been widely used. Both axial and beam elements may be used. Axial elements are assume to be pin connected with two degrees of freedom at nodal points while for the beam elements three degrees of freedom are assigned at the ends.

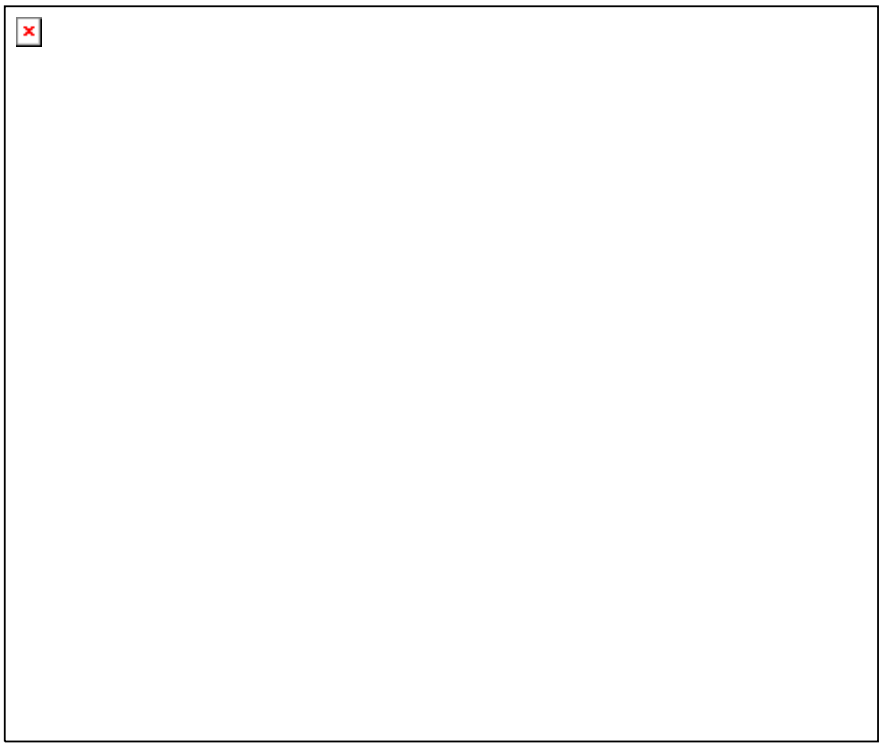

The discrete representation, in addition to its simplicity, has a significant advantage of accounting for possible displacement of the reinforcement with respect to surrounding concrete. The main disadvantage of this technique is that it requires a very fine mesh to enable each bar to lie on a boundary of the brick element.

An embedded representation may be used in connection with high order isoparametric elements. The reinforcing bar is considered to act as an axial member built into the isoparametric element such that its displacements are consistent with those of the basic element. The main advantage of this technique is in placing the steel in its exact position irrespective of the choice of the mesh.

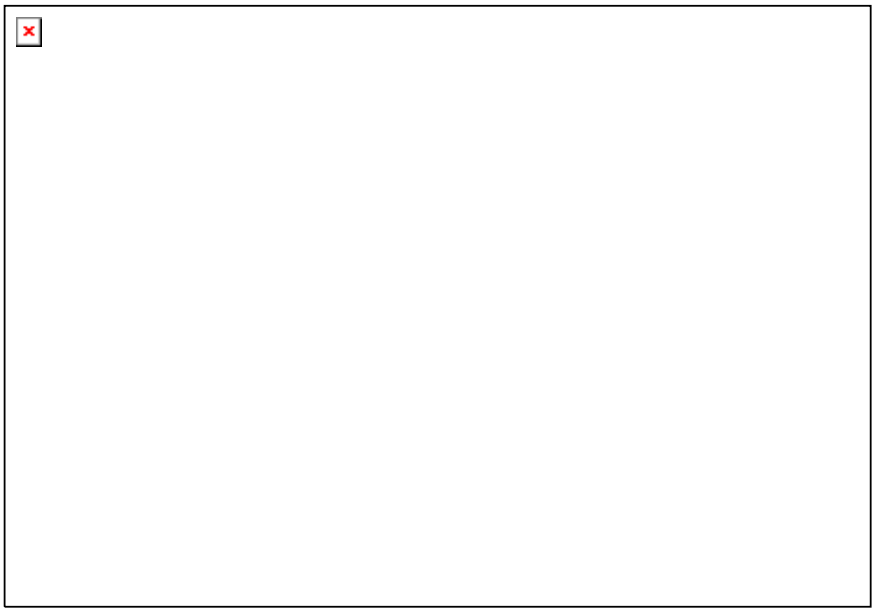

In this research one-dimensional discrete elements are employed to model reinforcement. This discrete form of representation is chosen due to its simplicity and its ability to account adequately for dowel action and bond slip mechanism. The main reinforcement is idealized by flexural elements (beam elements) since it is capable of resisting bending and direct shear.

The secondary reinforcement (side bars and web reinforcement) is idealized by axial elements (truss elements) the x-sectional area of such reinforcement is small and therefore its flexural rigidity maybe neglected.

4.6 Modeling of Concrete

A structural member whose thickness is small compared to its span or depth and is primarily loaded by in-plane forces can be model by two-dimensional elements. The stress state in such elements is defined in term of three stress components; σ_x, σ_y and σ_{xy}.

Stresses, normal to the plane of the elements, are considered negligible. Several types of plane stress elements are commonly used.

1- Constant triangular element

2- Plane isoparametric quadrilateral

3- High order isoparametric element

Constant triangular elements have enjoyed considerable appeal for their simplicity as well as their ability to idealize structure with irregular boundaries.

The main disadvantage of these elements stem from:

- Their uniform strain field and hence stress field; the stress results obtained usually require interpretation and averaging
- Mesh-dependency, a structural response obtained from certain mesh configuration may differ from that obtained from other meshes.

Isoparametric quadrilateral element have enjoyed for increase the mesh size and reduces the number of degrees of freedom, which results in significant reduction of computational effort. Also improved stress values can be obtained since the strains, and therefore the stresses, vary linearly within each element.

The main disadvantage of these elements is their poor behavior in representing pure bending.

4.6.1 Plane Isoparametric Quadrilateral:

The quadrilateral considered here has eight degrees of freedom; each node has two degree of freedom, u_{xi} and u_{yi}. The element has local coordinate system *s*-*t*, which is non-dimensional: *s* and *t* vary from -1 to 1.

Fig. 4.4 Plane Stress Linear Isoparametric quadrilateral Element

The local and global coordinate systems are related as follows:

$$X = \sum h_i x_i$$
$$Y = \sum h_i y_i$$

Where

X, Y = The global coordinates.
x_i, y_i = The local coordinates.
h_i = Interpolation function.

$$X = h_1 x_1 + h_2 x_2 + h_3 x_3 + h_4 x_4$$

$$Y = h_1 y_1 + h_2 y_2 + h_3 y_3 + h_4 y_4$$

$$\begin{vmatrix} X \\ Y \end{vmatrix} = \begin{vmatrix} h_1 & 0 & h_2 & 0 & h_3 & 0 & h_4 & 0 \\ 0 & h_1 & 0 & h_2 & 0 & h_3 & 0 & h_4 \end{vmatrix} \begin{vmatrix} x_1 \\ y_1 \\ x_2 \\ y_2 \\ x_3 \\ y_3 \\ x_4 \\ y_4 \end{vmatrix} \quad \text{……..……..4.1}$$

h_i is defined as:

$$h_1 = \frac{(1-s)(1-t)}{4}$$

$$h_2 = \frac{(1+s)(1-t)}{4}$$

$$h_3 = \frac{(1+s)(1+t)}{4}$$

$$h_4 = \frac{(1-s)(1+t)}{4}$$

General representation for interpolation function can be written as follows:

$$h_i = \frac{(1+s*s_i)(1+t*t_i)}{4} \quad \text{.....4.2}$$

Where (s,t) are the coordinates of node i

The above interpolation functions can also be used to define displacement within the element (Local system) in term of nodal displacements (global system).

$$U_X = \sum_{i=1}^{4} h_i u_{xi}$$

$$U_Y = \sum_{i=1}^{4} h_i \, u_{yi}$$

$$U_X = h_1 u_{x1} + h_2 u_{x2} + h_3 u_{x3} + h_4 u_{x4}$$

$$U_Y = h_1 u_{y1} + h_2 u_{y2} + h_3 u_{y3} + h_4 u_{y4}$$

$$\begin{vmatrix} U_X \\ U_Y \end{vmatrix} = \begin{vmatrix} h_1 & 0 & h_2 & 0 & h_3 & 0 & h_4 & 0 \\ 0 & h_1 & 0 & h_2 & 0 & h_3 & 0 & h_4 \end{vmatrix} \begin{vmatrix} u_{x1} \\ u_{y1} \\ u_{x2} \\ u_{y2} \\ u_{x3} \\ u_{y3} \\ u_{x4} \\ u_{y4} \end{vmatrix} \quad \text{……...……..4. 3}$$

Formulation of strain-displacement for two-dimensional deformation can be written as:

$$\varepsilon_x = \frac{\partial U_X}{\partial x} = \left(\frac{\partial h_i}{\partial x}\right)\ u_{xi} = h_{i,x} u_{xi}$$

$$\varepsilon_y = \frac{\partial U_Y}{\partial y} = \left(\frac{\partial h_i}{\partial y}\right) u_{yi} = h_{i,y} u_{yi}$$

$$\varepsilon_{xy} = \frac{\partial U_X}{\partial y} + \frac{\partial U_Y}{\partial x} = \left(\frac{\partial h_i}{\partial y}\right) u_{xi} + \left(\frac{\partial h_i}{\partial x}\right) u_{yi} = h_{i,y} u_{xi} + h_{i,x} u_{yi}$$

$$\begin{vmatrix} \varepsilon_x \\ \varepsilon_y \\ \varepsilon_{xy} \end{vmatrix} = \begin{vmatrix} \frac{\partial h_1}{\partial x} & 0 & \frac{\partial h_2}{\partial x} & 0 & \frac{\partial h_3}{\partial x} & 0 & \frac{\partial h_4}{\partial x} & 0 \\ 0 & \frac{\partial h_1}{\partial y} & 0 & \frac{\partial h_2}{\partial y} & 0 & \frac{\partial h_3}{\partial y} & 0 & \frac{\partial h_4}{\partial y} \\ \frac{\partial h_1}{\partial y} & \frac{\partial h_1}{\partial x} & \frac{\partial h_2}{\partial y} & \frac{\partial h_2}{\partial x} & \frac{\partial h_3}{\partial y} & \frac{\partial h_3}{\partial x} & \frac{\partial h_4}{\partial y} & \frac{\partial h_4}{\partial x} \end{vmatrix} \begin{vmatrix} u_{x1} \\ u_{y1} \\ u_{x2} \\ u_{y2} \\ u_{x3} \\ u_{y3} \\ u_{x4} \\ u_{y4} \end{vmatrix} \quad \text{……..……...……4.4}$$

Subsequently, we will need to express the derivatives of function in x,y coordinates in terms of its derivatives in s,t coordinates. This is done as follows: A function $f(x,y)$ can be considered to be an implicit function of s and t as $f=f[x(s,t),y(s,t)]$. Using the chain rule of differential, we have

$$\frac{\partial f}{\partial s} = \left(\frac{\partial f}{\partial x}\right)\left(\frac{\partial x}{\partial s}\right) + \left(\frac{\partial f}{\partial y}\right)\left(\frac{\partial y}{\partial s}\right)$$

$$\frac{\partial f}{\partial t} = \left(\frac{\partial f}{\partial x}\right)\left(\frac{\partial x}{\partial t}\right) + \left(\frac{\partial f}{\partial y}\right)\left(\frac{\partial y}{\partial t}\right)$$

$$\begin{vmatrix} \frac{\partial f}{\partial s} \\ \frac{\partial f}{\partial t} \end{vmatrix} = J \begin{vmatrix} \frac{\partial f}{\partial x} \\ \frac{\partial f}{\partial y} \end{vmatrix} \quad \text{.....4.5}$$

Where

J=Jacobian matrix to transfer variable from x-y plane to s-t plane.

$$J = \begin{vmatrix} x_i\left(\frac{\partial h_i}{\partial s}\right) & y_i\left(\frac{\partial h_i}{\partial s}\right) \\ x_i\left(\frac{\partial h_i}{\partial t}\right) & y_i\left(\frac{\partial h_i}{\partial t}\right) \end{vmatrix} \quad \text{.....4.6}$$

$$J = \begin{vmatrix} \frac{\partial h_1}{\partial s} & \frac{\partial h_2}{\partial s} & \frac{\partial h_3}{\partial s} & \frac{\partial h_4}{\partial s} \\ \frac{\partial h_1}{\partial t} & \frac{\partial h_2}{\partial t} & \frac{\partial h_3}{\partial t} & \frac{\partial h_4}{\partial t} \end{vmatrix} \begin{vmatrix} x_1 & y_1 \\ x_2 & y_2 \\ x_3 & y_3 \\ x_4 & y_4 \end{vmatrix} \quad \text{.....4.7}$$

$$J = \begin{vmatrix} J_{11} & J_{12} \\ J_{21} & J_{22} \end{vmatrix} \quad \text{.....4.8}$$

$$J = \frac{1}{4} \begin{vmatrix} -(1-t)x_1 - (1+t)x_2 + (1+t)x_3 + (1-t)x_4 & -(1-t)y_1 - (1+t)y_2 + (1+t)y_3 + (1-t)y_4 \\ -(1-s)x_1 - (1+s)x_2 + (1+s)x_3 + (1-s)x_4 & -(1-s)y_1 - (1+s)y_2 + (1+s)y_3 + (1-s)y_4 \end{vmatrix} \quad \text{.....4.9}$$

$$\begin{vmatrix} \frac{\partial f}{\partial x} \\ \frac{\partial f}{\partial y} \end{vmatrix} = \frac{1}{\det J} \begin{vmatrix} J_{22} & -J_{12} \\ -J_{21} & J_{11} \end{vmatrix} \begin{vmatrix} \frac{\partial f}{\partial s} \\ \frac{\partial f}{\partial t} \end{vmatrix} \quad \text{.....4.10}$$

$$\det j = (j_{22} * j_{11}) - (j_{12} * j_{21}) \quad \text{.....4.11}$$

$$dxdy = \det j dsdt \quad \text{.....4.12}$$

A major disadvantage of linear isoparametric quadrilateral is its poor behavior under pure bending as shown in fig.4.5. This involves the addition to displacement fields, defined by eq.(4.13) and eq.(4.14) corrective displacement function of the form:

$$U_X = \alpha_1(1-s^2)+\alpha_2(1-t^2) \quad \text{.....4.13}$$

$$U_Y = \alpha_3(1-s^2)+\alpha_4(1-t^2) \quad \text{.....4.14}$$

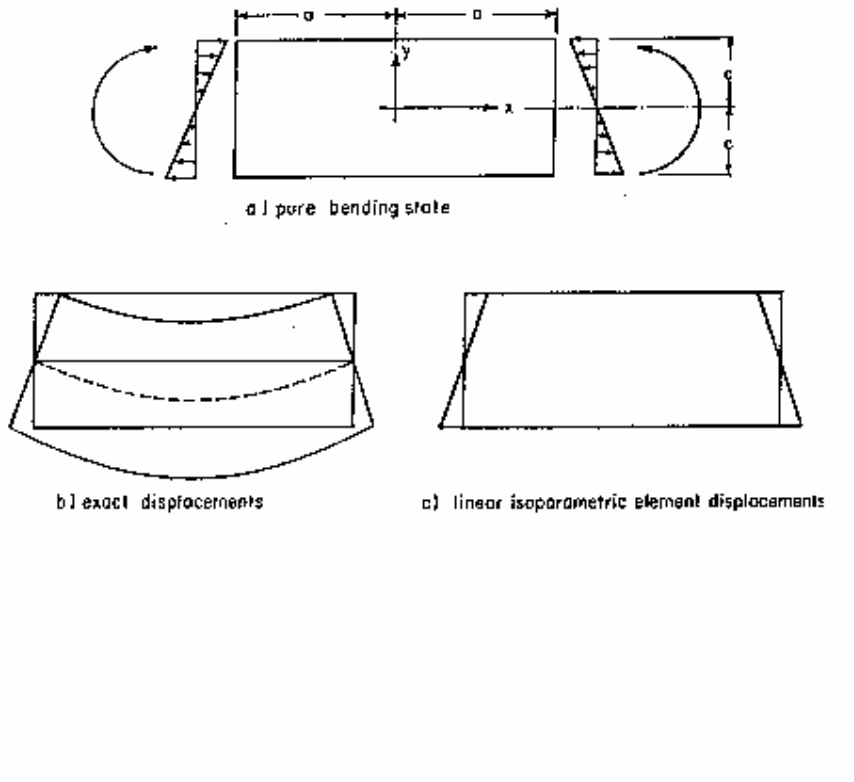

Complete displacement field of the improved element is as follows:

$$U_X = \sum_{i=1}^{4} h_i u_{xi} + \alpha_1(1-s^2) + \alpha_2(1-t^2) \quad \text{.....4.15}$$

$$U_Y = \sum_{i=1}^{4} h_i u_{yi} + \alpha_3(1-s^2) + \alpha_4(1-t^2) \quad \text{.....4.16}$$

Where

$\alpha_1, \alpha_2, \alpha_3, \alpha_4$ =The constants which constitute additional degrees of freedom.

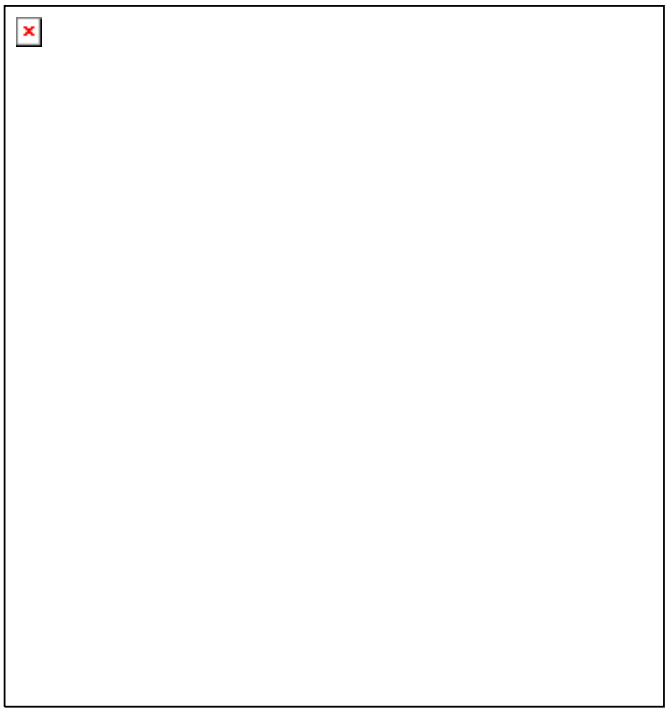

The additional degrees of freedom increase the size of stiffness matrix to12×12.Since α_1, α_4 constitute displacement amplitudes relative to the displacements of the corner nodes; they can be condensed by minimizing the strain energy on the element level. To achieve this, the static condensation method can be used by partitioning the12×12 stiffness matrix:

$$\begin{vmatrix} P_1 \\ P_2 \end{vmatrix} = \begin{vmatrix} K_{11} & K_{12} \\ K_{21} & K_{22} \end{vmatrix} \begin{vmatrix} U \\ \alpha \end{vmatrix} \quad \text{.....4.17}$$

$$[P_1] = [K_{11}]U + [K_{12}][\alpha] \quad \text{.....4.18}$$

$$[P_2] = [K_{21}]U + [K_{22}][\alpha] \quad \text{.....4.19}$$

The strain energy of the element is:

$$S.E = \tfrac{1}{2}\begin{vmatrix} U^T & \| & K_{11} & K_{12} \| U \\ \alpha & \| & K_{21} & K_{22} \| \alpha \end{vmatrix} \quad \text{.....4.20}$$

For minimum strain energy:

$$\tfrac{\partial S.E}{\partial \alpha} = 0 = [K_{21}]|U| + [K_{22}]|\alpha| \quad \text{.....4.21}$$

$$|\alpha| = [K_{22}]^{-1}[K_{21}]|U| \quad \text{.....4.22}$$

By substituting eq.(4.22) into eq.(4.18) we can obtain the following expression:

$$|P_1| = ([K_{11}] - [K_{12}][K_{22}]^{-1}[K_{21}])|U| \quad \text{.....4.23}$$

$$|P_1| = [K]|U| \quad \text{.....4.24}$$

Where $[K]$=8×8 modified stiffness matrix

$$[K] = \sum_i \sum_j w_i w_j J[B(s_i, t_i)]^T [C][B(s_i, t_i)] \quad \text{.....4.25}$$

Where

s_i, t_i = Integration points.

w_i, w_j = Weight factors corresponding to s_i, t_i.

C= Material stiffness matrix.

$B(s_i, t_i)$=Strain displacement matrix.

4.6.2 Constant Strain Triangular Element

The Plane triangular element considered here has six degrees of freedom. Each node has two degrees of freedom. The numbering of nodes counterclockwise is shown in Fig.4.7.

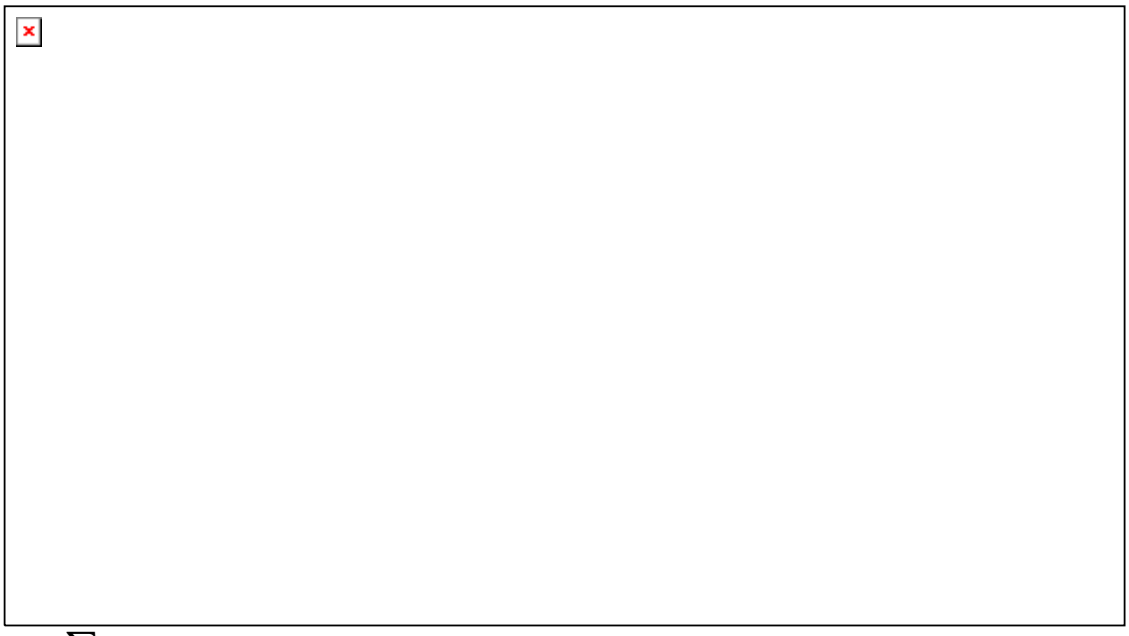

$$X = \sum N_i x_i$$

$$Y = \sum N_i y_i$$

$$Y = N_1 y_1 + N_2 y_2 + N_3 y_3$$

$$\begin{vmatrix} X \\ Y \end{vmatrix} = \begin{vmatrix} N_1 & 0 & N_2 & 0 & N_3 & 0 \\ 0 & N_1 & 0 & N_2 & 0 & N_3 \end{vmatrix} \begin{vmatrix} x_1 \\ y_1 \\ x_2 \\ y_2 \\ x_3 \\ y_3 \end{vmatrix} \quad \text{……..……..4.26}$$

Where

N_i= Shape function.

$$N_i = (\alpha_i + \beta_i x + \gamma_i y)/2A_e \quad \text{……4.27}$$

$i=1,2,3$

$$\alpha_i = x_j y_k - x_k y_j \quad \text{……...……4.28}$$

$$\beta_i = y_i - y_k \text{ ……..……..4.29}$$

$$\gamma_i = x_k - x_j \text{ …...……..4.30}$$

$$u_x = a_1 + a_2 x + a_3 y$$
$$u_y = a_4 + a_5 x + a_6 y$$

$$\begin{vmatrix} 1 & x_1 & y_1 \\ 1 & x_2 & y_2 \\ 1 & x_3 & y_3 \end{vmatrix} \begin{vmatrix} a_1 \\ a_2 \\ a_3 \end{vmatrix} = \begin{vmatrix} u_{x1} \\ u_{x2} \\ u_{x3} \end{vmatrix} \text{ ……4.31}$$

$$a_1 = [u_1(x^2 y^3 - x^3 y^{\ 2}) + u_2(x^3 y^1 - x^1 y^3) + u_3(x_1 y_2 - x_2 y_1)] / 2A_e$$
$$a_2 = [u_1(y_2 - y_3) + u_2(y_3 - y_1) + u_3(y_1 - y_2)] / 2A_e$$
$$a_3 = [u_1(x_3 - x_2) + u_2(x_1 - x_3) + u_3(x_2 - x_1)] / 2A_e$$

$$\begin{vmatrix} 1 & x_1 & y_1 \\ 1 & x_2 & y_2 \\ 1 & x_3 & y_3 \end{vmatrix} \begin{vmatrix} a_4 \\ a_5 \\ a_6 \end{vmatrix} = \begin{vmatrix} u_{y1} \\ u_{y2} \\ u_{y3} \end{vmatrix} \text{ ……4.32}$$

$$2A_e = \begin{vmatrix} 1 & x_1 & y_1 \\ 1 & x_2 & y_2 \\ 1 & x_3 & y_3 \end{vmatrix} \text{ ……4.33}$$

$$a_4 = [u_4(x_2 y_3 - x_3 y_2) + u_5(x_3 y_1 - x_1 y_3) + u_6(x_1 y_2 - x_2 y_1)] / 2A_e$$
$$a_5 = [u_4(y_2 - y_3) + u_5(y_3 - y_1) + u_6(y_1 - y_2)] / 2A_e$$
$$a_6 = [u_4(x_3 - x_2) + u_5(x_1 - x_3) + u_6(x_2 - x_1)] / 2A_e$$

$$2A_e = (x_2 y_3 - x_3 y_2) + (x_3 y_1 - x_1 y_3) + (x_1 y_2 - x_2 y_{1)}$$

The displacement function U_X,U_Y can be expressed in terms of nodal displacements as follow:

$$\begin{vmatrix} U_X \\ U_Y \end{vmatrix} = \begin{vmatrix} N_1 & 0 & N_2 & 0 & N_3 & 0 \\ 0 & N_1 & 0 & N_2 & 0 & N_3 \end{vmatrix} \begin{vmatrix} u_{x1} \\ u_{y1} \\ u_{x2} \\ u_{y2} \\ u_{x3} \\ u_{y3} \end{vmatrix} \text{.....4.34}$$

Formulation of strain-displacement for two-dimensional deformation can be written as follows:

$$\varepsilon_x = \frac{\partial u_x}{\partial x} = \frac{\partial N_i}{\partial x} u_{xi} = N_{i,x} u_{xi}$$

$$\varepsilon_y = \frac{\partial u_y}{\partial y} = \frac{\partial N_i}{\partial x} u_{yi} = N_{i,x} u_{yi}$$

$$\varepsilon_{xy} = \frac{\partial u_x}{\partial y} + \frac{\partial u_y}{\partial x} = \frac{\partial N_i}{\partial y} u_{xi} + \frac{\partial N_i}{\partial x} u_{yi} = N_{i,y} u_{xi} + N_{i,x} u_{yi}$$

$$\begin{vmatrix} \frac{\partial N_1}{\partial x} & 0 & \frac{\partial N_1}{\partial x} & 0 & \frac{\partial N_1}{\partial x} & 0 & \frac{\partial N_1}{\partial x} & 0 \\ 0 & \frac{\partial N_1}{\partial x} & 0 & \frac{\partial N_1}{\partial x} & 0 & \frac{\partial N_1}{\partial x} & 0 & \frac{\partial N_1}{\partial x} \\ \frac{\partial N_1}{\partial x} & \frac{\partial N_1}{\partial x} & \frac{\partial N_1}{\partial x} & \frac{\partial N_1}{\partial x} & \frac{\partial N_1}{\partial x} & \frac{\partial N_1}{\partial x} & \frac{\partial N_1}{\partial x} & \frac{\partial N_1}{\partial x} \end{vmatrix} \begin{vmatrix} u_{x1} \\ u_{y1} \\ u_{x2} \\ u_{y2} \\ u_{x3} \\ u_{y3} \end{vmatrix} = \begin{vmatrix} \varepsilon_x \\ \varepsilon_y \\ \varepsilon_{xy} \end{vmatrix} \text{.....4.35}$$

$$\frac{\partial f}{\partial s} = \frac{\partial f}{\partial x}\frac{\partial x}{\partial s} + \frac{\partial f}{\partial y}\frac{\partial y}{\partial s}$$

$$\frac{\partial f}{\partial t} = \frac{\partial f}{\partial x}\frac{\partial x}{\partial t} + \frac{\partial f}{\partial y}\frac{\partial y}{\partial t}$$

$$\begin{vmatrix} \frac{\partial f}{\partial s} \\ \frac{\partial f}{\partial t} \end{vmatrix} = J \begin{vmatrix} \frac{\partial f}{\partial x} \\ \frac{\partial f}{\partial y} \end{vmatrix} \text{.....4.36}$$

$$J = \begin{vmatrix} (\frac{\partial x}{\partial s}) & (\frac{\partial y}{\partial s}) \\ (\frac{\partial x}{\partial t}) & (\frac{\partial y}{\partial t}) \end{vmatrix} \text{……..……...……..4.37}$$

$$J = \begin{vmatrix} x_i(\frac{\partial N_i}{\partial s}) & y_i(\frac{\partial N_i}{\partial s}) \\ x_i(\frac{\partial N_i}{\partial t}) & y_i(\frac{\partial N_i}{\partial t}) \end{vmatrix} \text{……..…….4.38}$$

$$\det j = (x_1 - x_3)(y_2 - y_3) - (x_2 - x_3)(y_1 - y_3) \text{ ……..……....4.39}$$

$$dxdy = \det j dsdt \text{ ……4.40}$$

From the knowledge of the area of triangle, it can see that the magnitude of *det J* is twice the area of the triangle. If points 1, 2, 3 are ordered in counterclockwise manner, det *J* is positive in sign. We have:

$$A = 0.5 \det j \text{ ……4.41}$$

In this research plane isoparametric quadrilaterals with eight degree of freedom will be adopted. A modified version of this element is used to improved behavior under pure bending.

4.7 Modeling of Link Elements

Two-dimensional link elements having two orthogonal fictitious springs are used to model the bond slip, aggregate interlock and dowel action phenomena. Ngo and Scordelis introduced firstly the link element to allow a slip relationship between two initially coincident nodes. Fig.4.8 below shows such an element oriented at some angle θ relative to the global coordinate system.

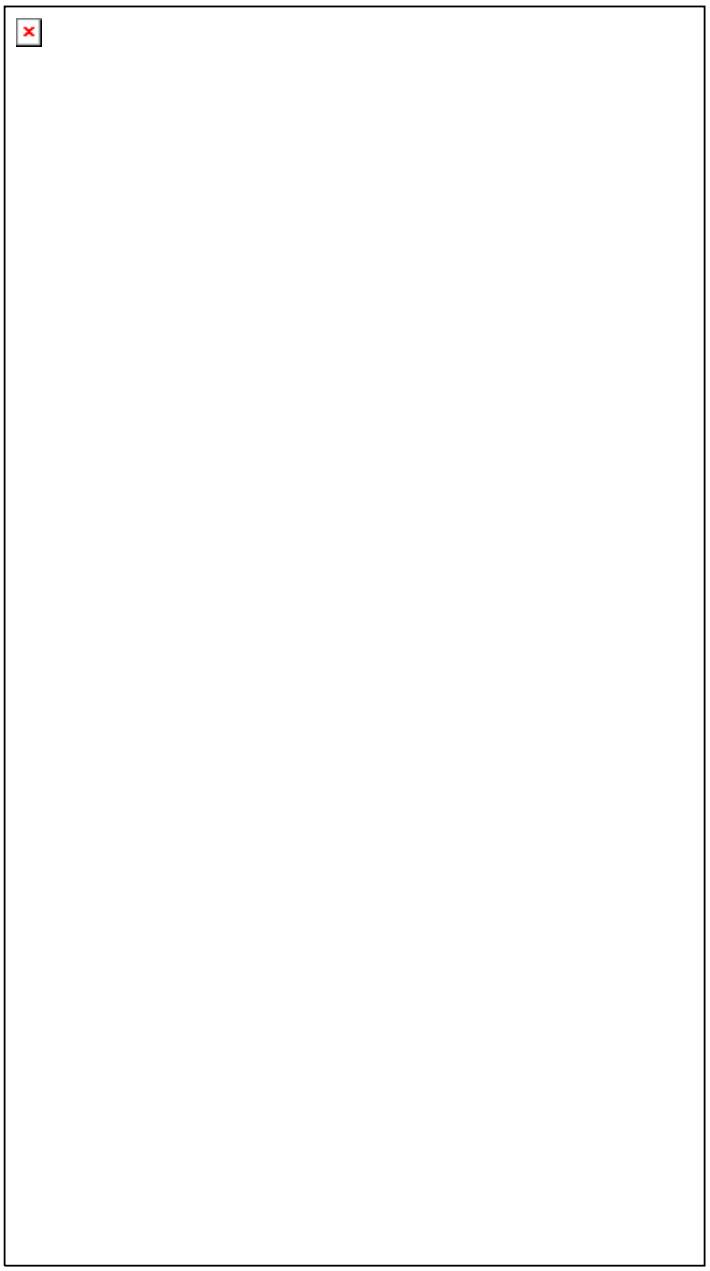

The stiffness matrix K in global coordinates is:

$$K = \begin{vmatrix} k_{11} & -k_{11} & k_{12} & -k_{12} \\ -k_{11} & k_{11} & -k_{12} & k_{12} \\ k_{12} & -k_{12} & k_{22} & -k_{22} \\ -k_{12} & k_{12} & -k_{22} & k_{22} \end{vmatrix} \quad \text{.....4.42}$$

Where

$$k_{11} = k_h \cos^2\theta + k_v \sin^2\theta \quad \text{.....4.43}$$

$$k_{12} = (k_h - k_v)\cos\theta\sin\theta \quad \text{.....4.44}$$

$$k_{22} = k_h \sin^2\theta + k_v \cos^2\theta \quad \text{.....4.45}$$

The link stiffness matrix is general and can be applied to any of the phenomenon mentioned above by assigning appropriate stiffness value.

4.8 Modeling of Cracking

One of important source of material non-linearity in reinforced concrete member is cracking of concrete. However, an adequate representation of cracking in finite element mode required considerable effort. This is due to difficulty, which arises from the continued propagation of cracks with increasing load.

Most reinforced concrete finite element models have been developed according to two distinct cracking representation methods:

- Discrete cracking method.
- Distributed cracking method.

4.8.1 Discrete Crack Method

In the first method the displacement discontinuities across crack are accounted for by disconnecting elements at nodal points along their boundaries as shown in Fig. 4.9.

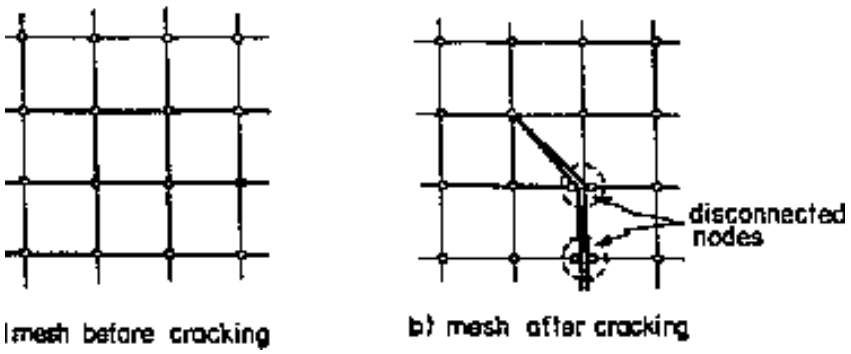

Fig. 4.9 Discrete Crack Representation

The main problem in this approach, however, is the difficulty, which arises from introduction of additional nodal points required by altered topology of analytical model. These additional degrees of freedom result in greater bandwidth in

global stiffness matrix. This leads to an unjustifiable increase in the computational effort required to solve the stiffness equation.

There are two strategies by which this method of crack modeling may be implemented. In the first, the analysis is terminated when tensile cracking is detected. The topology of the structure is then redefined; the nodal points are renumbered such that the input data is updated to the new topology .The solution process is then continues until further cracking is detected. This strategy is lengthy and is considered impractical as an analytical tool.

The second strategy involves the definition of two or four nodes occupying the same coordinates in space as shown in Fig.4.10 and Fig4.11 respectively, these nodes are initially rigidly joined until cracking is detected in adjacent elements. When this occurs the nodes are released by reducing the stiffness of linkage to zero. In cases where the modeling of post-cracking shear resistance mechanisms is desired, these stiff linkages are replaced by ones corresponding to aggregate interlock and or dowel action.

One-Dimensional Cracking

Fig.4.10

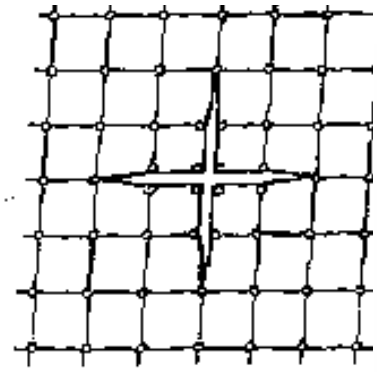

Two-Dimensional Cracking

Fig4.11

The difference between defining two or four nodes in probable cracking regions depends on the pattern of cracking anticipated. If the cracking is expected to develop in two directions, a situation that may arise from cyclic loading, for example then the four nodes must be used. One directional cracking, however, requires only two nodes. This situation generally is obtained in case where the load is increase monotonically to failure.

As the high stiffness values of linkages are reduced to stiffness values corresponding to aggregate interlock and/or dowel action linkages to release the rigidly connected nodes, the excess tensile forces in the linkages are converted into nodal forces, which will be referred to as unbalanced forces. These unbalanced forces are applied to the system in the next cycle (iteration) so as to distribute the excess tensile stresses to adjacent elements.

Advantage of discrete cracking can be summarized as follow:

1-It is more realistic representation of cracking.

2-It is better to simulate the aggregate interlock and dowel action mechanism.

The disadvantage of this type of representation:

1-It requires a continuously changing definition of topology as cracking progress.

2-Cracking direction is dependent on mesh geometry and the type of elements used.

4.8.2 Distributed Cracking Method

This method achieves a stress discontinuity state consistent with the existence of crack. When the principal tensile strain in an element exceeds a failure criterion, the stiffness of element is reduced to zero in the direction of principal strain. Elements are cracked in this manner are postulated to be incapable of carrying stresses normal to cracked direction see Fig.4.12. These stresses

are converted into nodal forces (unbalanced forces). These forces are applied to the structure in the next cycle (iteration) so as to distribute the released tensile forces to adjacent element.

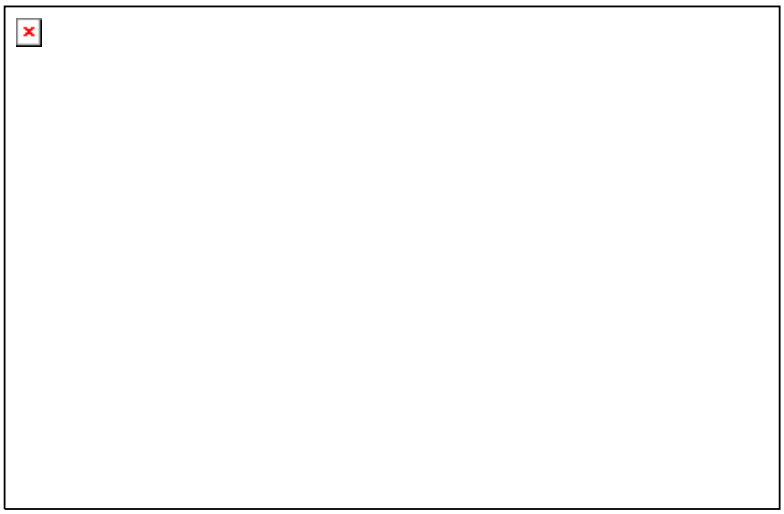

Advantage of distributed cracking:

1-No change in the topology as cracking progress.

2-Complete generality in regard to cracking direction, independent of mesh geometry and the type of elements used.

The main disadvantage of this method:

1-It cannot provide a realistic prediction of distribution of strain, and therefore stresses in region adjacent to cracks.

2-The aggregate interlock and dowel action mechanism cannot be realistically incorporated.

Both of these cracking representations are employed in this analysis either individually or simultaneously. The first is adopted for realistic modeling of dowel action and aggregate interlock mechanisms and the second, for the advantage of achieving automatic crack propagation with a relatively small effort.

4.9 Solution Strategy using an Incremental-Iterative Method

1- apply a load increment and analyze the structure using the updated stiffness matrix.

2- From the resulting displacement increments determined in the analysis of previous load increment, calculate the strain increments $(\delta\varepsilon_i)$ and add it to existing strains (ε_{i-1}).

$$\varepsilon_i = \varepsilon_{i-1} + \partial\varepsilon_i$$

3- from these strains calculates the stresses.

4- Using the current stresses and strains (σ_i, ε_i) check all the elements against any failure criterion.

5- Calculate new stiffness values.

6-For each element, calculate the unbalanced loads resulting from material failure or change in stiffness values.

7- Assemble the global unbalanced load vector.

8-Check the current displacement increments and or current unbalanced loads vector for convergence. If the solution converges or prespecified maximum number of iteration has been exceeded, go to step 1,if divergence is indicated, stop the solution.

9-If the solution has not converged or prespecified max.number of iteration has not been exceeded reanalyze the structure for unbalanced load vector. In this analysis the stiffness matrix used at the beginning of the load increment is employed. After obtaining the displacement-increment due to the unbalanced load go to step 2.

CHAPTER(5)
CONCRETE CONSITUTITIVE RELATIONS

5.1 Biaxial Stress-strain Relation-ship

In this research constitutive relation for concrete based on the analytical and experimental investigation of Lui and Tasuji[24] is used. An analytical characterizations in conjunction with experimental data are postulated to describe the behavior of concrete under a following biaxial state of stresses:

Tension-Tension

Tension-Compression

Compression-Compression

Material response is assumed to be orthotropic. The tangent stiffness values E_1 and E_2 corresponding to the principal strains ε_1 and ε_2 respectively are derived from a stress-strain relation advanced by Lui and Tasuji.

For elastic analysis stresses and the strains are related as follows:

$$\sigma = \frac{\varepsilon E}{1-\nu\alpha}$$

$$\begin{vmatrix}\sigma_1\\ \sigma_2\\ \sigma_{12}\end{vmatrix} = \frac{E}{1-\nu^2}\begin{vmatrix}1 & \gamma & 0\\ \gamma & 1 & 0\\ 0 & 0 & \frac{1-\nu}{2}\end{vmatrix}\begin{vmatrix}\varepsilon_1\\ \varepsilon_2\\ \varepsilon_{12}\end{vmatrix} \quad \text{.....5.1}$$

Where

E= Initial uniaxial modulus of elasticity.

ν= Poisson's ratio.

σ, ε= Stress and strain in one of principle direction.

α=Stresses-ratio; the ratio of the stress in perpendicular direction to that in the direction considered.

For non-linear analysis eq.(5.1) can be modified as follows:

$$\sigma = \frac{A + B\varepsilon E}{(1-\nu\alpha)(1+C\varepsilon+D\varepsilon^2)} \quad \text{.....5.2}$$

The constant A, B, C and D can be defined from the boundary condition as following:

$$A = 0$$

$$B = 1$$

$$C = \frac{E}{\sigma_p(1-\nu\alpha)} - \frac{2}{\varepsilon_p}$$

$$D = \frac{1}{\varepsilon_p^{\,2}}$$

$$\sigma = \frac{\varepsilon E}{(1-\nu\alpha)[1+(\frac{1}{1-\nu\alpha}\frac{E}{E_s}-2)(\frac{\varepsilon}{\varepsilon_p})+(\frac{\varepsilon}{\varepsilon_p})^2]}$$

$$\begin{vmatrix}\sigma_1\\ \sigma_2\\ \sigma_{12}\end{vmatrix} = \begin{vmatrix}\lambda\frac{E_1}{E_2} & \lambda\nu_1 & 0\\ \lambda\nu_1 & \lambda & 0\\ 0 & 0 & \frac{E_1E_2}{E_1+E_2+2E_2\gamma_1}\end{vmatrix}\begin{vmatrix}\varepsilon_1\\ \varepsilon_2\\ \varepsilon_{12}\end{vmatrix} \quad \text{.....5.3}$$

Where

E_s = Secant modulus of elasticity at peak stress.

σ_p , ε_p = Stress and strain at peak point.

$E, \varepsilon_p, \nu, \sigma_p$ are the unknowns in eq. (5.3) and they can be obtained from experimental data.

$$E_s = \frac{\sigma_p}{\varepsilon_p} \quad \text{.....5.4}$$

$$\lambda = \frac{E_1}{(\frac{E_1}{E_2} - \nu_1^{\,2})} \quad \text{.....5.5}$$

$$E_i = \frac{d\sigma_i}{d\varepsilon_i} = \frac{E[1-(\frac{\varepsilon_i}{\varepsilon_p})^2]}{[1+(\frac{1}{1-\nu\alpha_1}\frac{E}{E_s}-2)(\frac{\varepsilon_i}{\varepsilon_p})+(\frac{\varepsilon_i}{\varepsilon_p})^2]^2} \quad \text{.....5.6}$$

$$\sigma_i' = (1-\nu\alpha_i)\sigma_i \quad \text{.....5.7}$$

Where i=1,2

5.2 Biaxial Stress Failure Envelope and Corresponding Strains

To establish a valid failure criterion for plain concrete in all combinations of biaxial stress, an experimental investigation was conducted by Tasuji et al [24]. This work is an earlier extension of experimental investigation by Lui et al[25] limited to the biaxial compression state of stress.

From the test result obtained, a biaxial failure envelope was developed as shown in Fig.5.1.

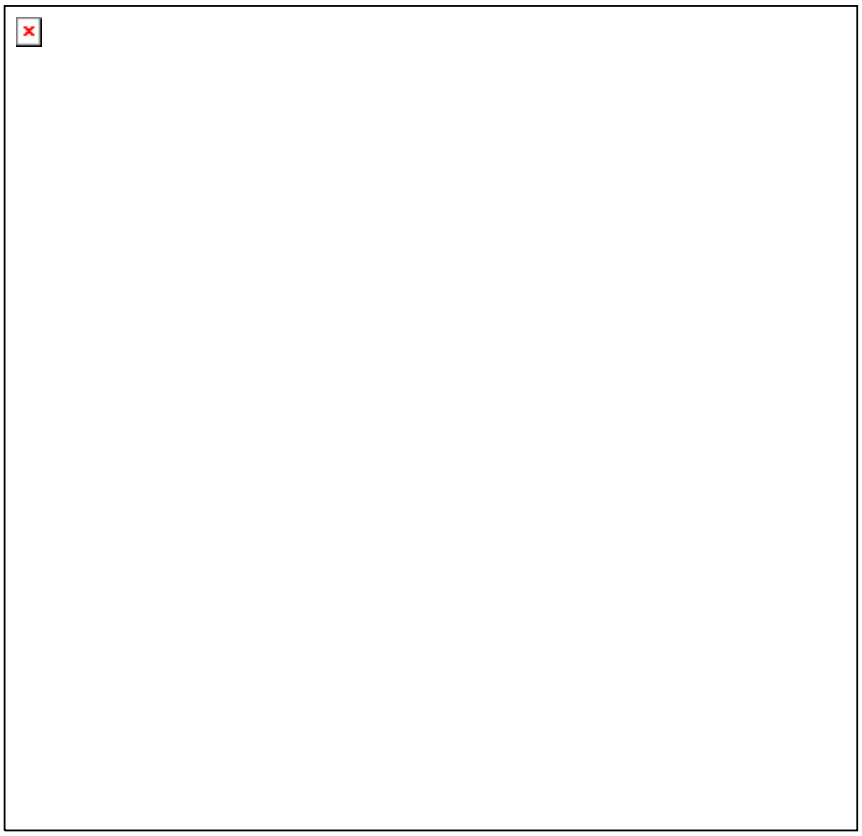

For purpose of simplicity, a bi-linear approximation of the envelope was suggested as shown in Fig.5.2

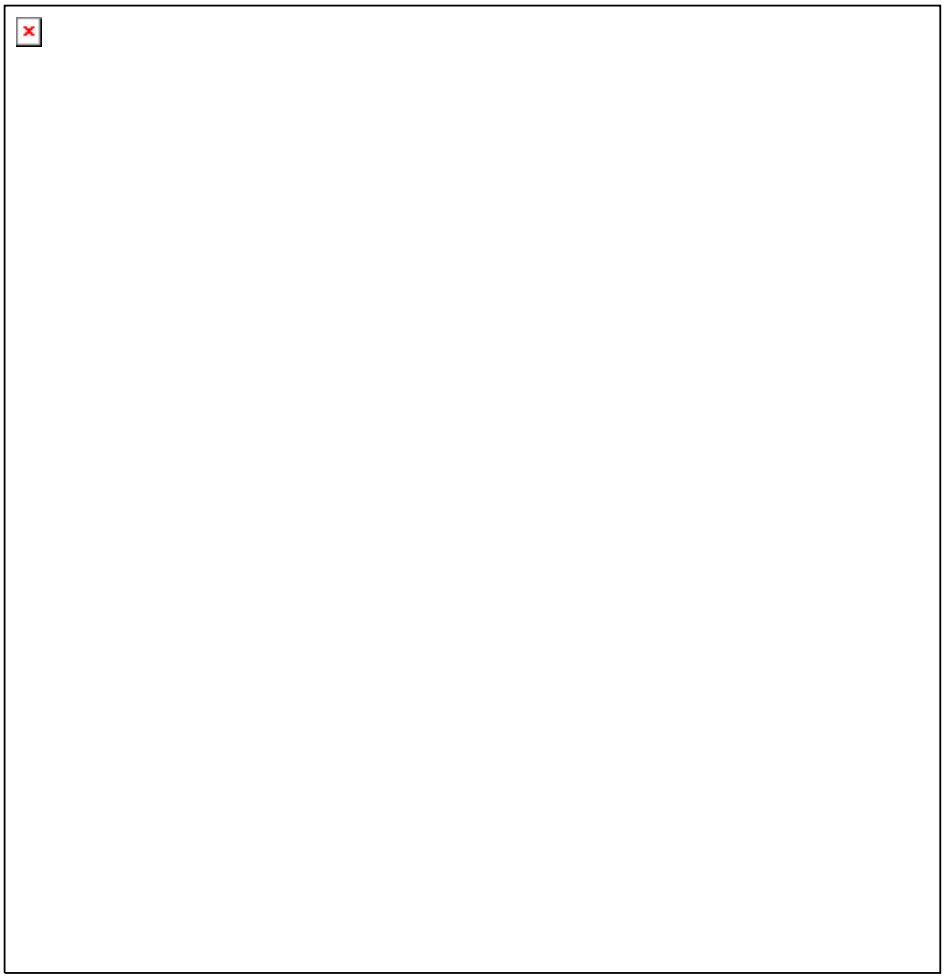

Also Tasuji obtained strain values corresponding to peak stresses in three regions of biaxial stress as shown in Fig.5.3.These strain values are approximated by straight lines using method of least square (these approximations are applicable only to the range of biaxial stress ratios tested).

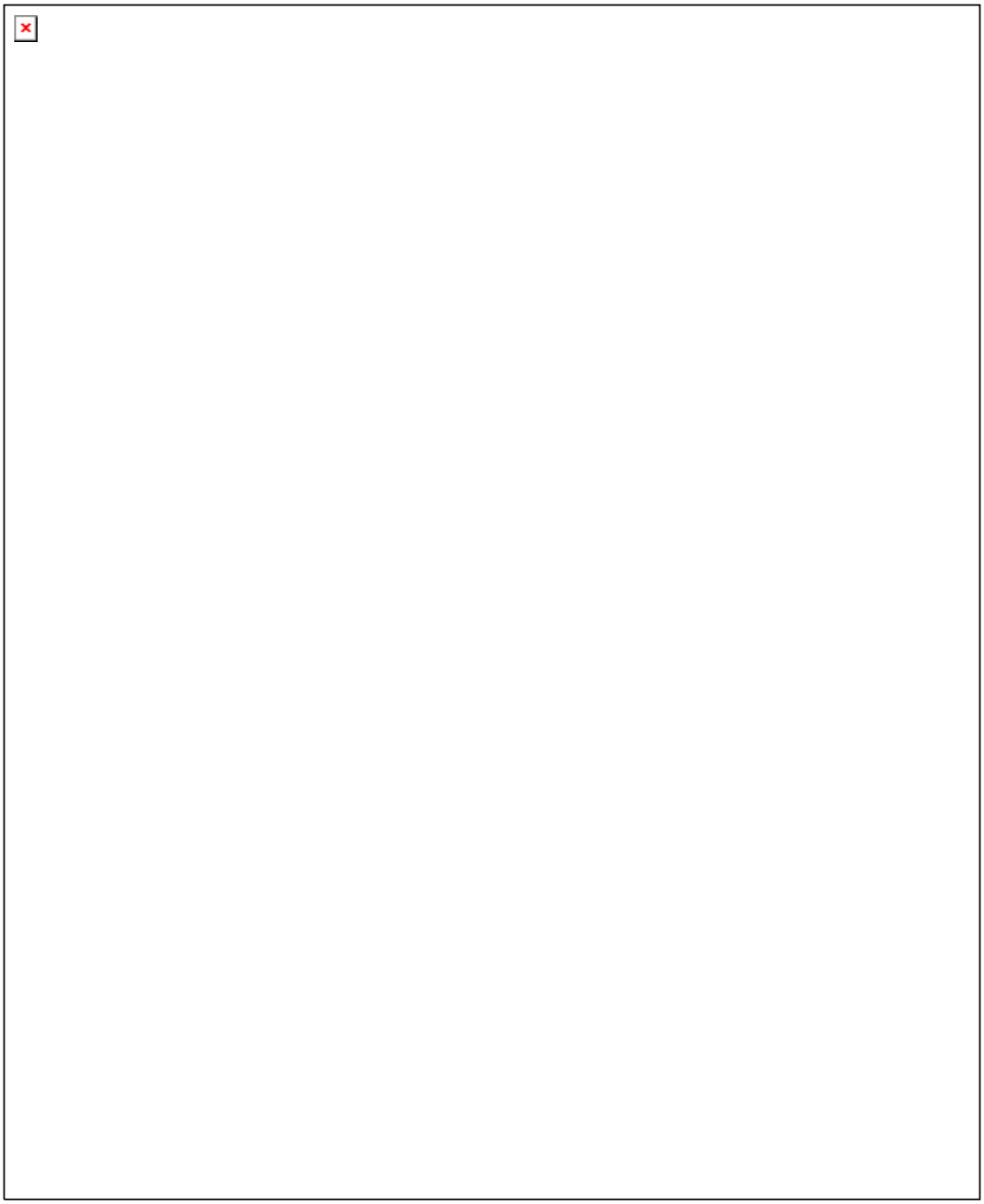

The strain values are expressed in term of $\sigma_p/\sigma_{c0,}\sigma_p/\sigma_{t0}$ for compression and tension direction respectively.Fig.5.4 and Fig.5.5 give the relation between these strains and peak stresses for the two directions.

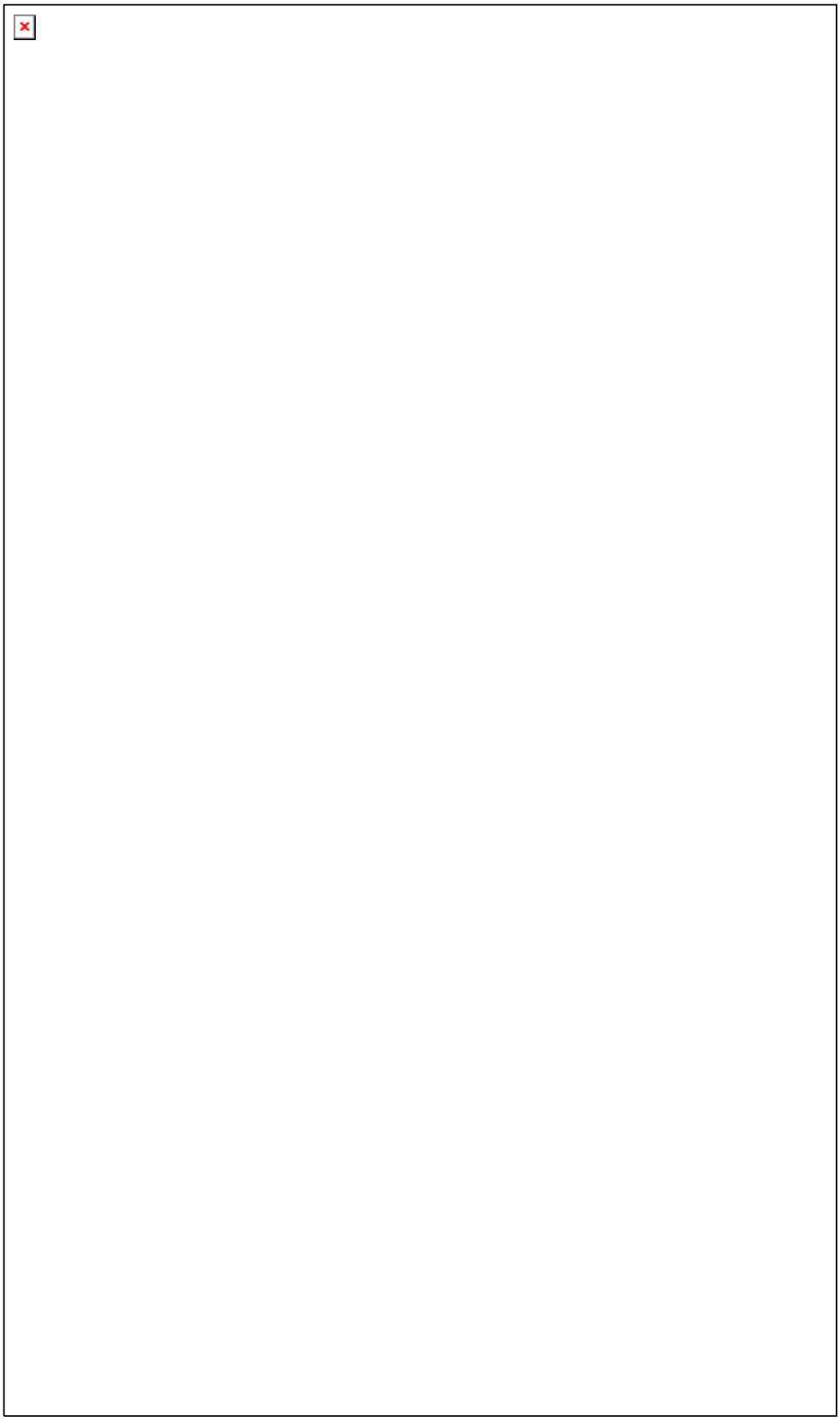

The adjusted strain values represented by dotted lines can be expressed in terms of the strain ε_{pc}, ε_{pt} corresponding to uniaxial peak stress in compression and tension respectively.

5.2.1 Biaxial Compression-Compression

$$\varepsilon_p = (0.76 + \frac{\varepsilon_{pc} \times 1000 - 0.76}{\alpha_1}) \times 10^{-3} \quad \text{.....5.8}$$

(Direction of absolute minimum compression)

$$\varepsilon_P = \varepsilon_{Pc} \quad \text{.....5.9}$$

(Direction of absolute maximum compression)

5.2.2 Biaxial Compression-Tension

$$\varepsilon_p = (1.18 + \frac{1.18 - \varepsilon_{pt} \times 1000}{1 + \alpha_1 \frac{\sigma_{t0}}{\sigma_{c0}}}) \times 10^{-3} (Tension) \quad \text{.....5.10}$$

$$\varepsilon_p = (-0.36 + \frac{\varepsilon_{pc} \times 1000 + .36}{1 + \alpha_2 \frac{\sigma_{c0}}{\sigma_{t0}}}) \times 10^{-3} (Compression) \quad \text{.....5.11}$$

5.2.3 Biaxial Tension-Tension

$$\varepsilon_p = \varepsilon_{pt} \quad \text{.....5.12}$$

(in direction of maximum tension)

$$\varepsilon_p = (0.026 + \frac{\varepsilon_{pt} \times 1000 + 0.026}{\alpha_2}) \times 10^{-3} \quad \text{.....5.13}$$

(in direction of minimum tension)

Where

$$\alpha_1 = \frac{\sigma_2}{\sigma_1} \quad \text{.....5.14}$$

$$\alpha_2 = \frac{\sigma_1}{\sigma_2} \quad \text{.....5.15}$$

$\sigma_{t0}, \varepsilon_{pt}$= Uniaxial tensile stress and strain respectively at peak point.

$\sigma_{c0}, \varepsilon_{pc}$= Uniaxial compressive stress and strain respectively at peak point.

5.3 Failure Criteria

The criteria used to detect failure are based on strains corresponding to peak stresses. Material failure can be detected by checking principal strain against their limiting values.

Principal strains can be obtain according to the following iterative procedure suggested by Cedolin and Dei Poli[24]:

1- Estimate σ_1, σ_2 from $\varepsilon_1, \varepsilon_2$ by using E_1, E_2 from previous load increment or iteration.
2- Find the stress ratio α_1, α_2 by substituting values of σ_1, σ_2 in eq. (5.3).
3- Produced a new values of σ_1, σ_2 from eq.(5.14) and eq.(5.15)

these steps are repeated until we reached the correct value of σ_1, σ_2.

Failure is defined as follows:

5.3.1 Tension-Tension

In this stress state, principal strains $\varepsilon_1, \varepsilon_2$ are positive and checked against limiting values given by eq.(5.12) and eq. (5.13) respectively.

If $\varepsilon_1 > \varepsilon_p$(limiting value)then $E_1 = 0$(Cracking has occurred and material is not capable of carrying stresses in this direction).

The stress-strain relation-ship.

$$\begin{vmatrix} \sigma_1 \\ \sigma_2 \\ \sigma_{12} \end{vmatrix} = \begin{vmatrix} 0 & 0 & 0 \\ 0 & E_2 & 0 \\ 0 & 0 & \overline{G} \end{vmatrix} \begin{vmatrix} \varepsilon_1 \\ \varepsilon_2 \\ \varepsilon_{12} \end{vmatrix} \quad \text{.....5.16}$$

Where

E_2=Uniaxial tangent modulus of elasticity can be obtained from eq.(5.6)by substituting $\alpha = 0$

G= Reduced shear modulus of elasticity to account for the post cracking aggregate interlock.

Also if $\varepsilon_2 > \varepsilon_p$ then $E_2 = 0$

5.3.2 Tension-Compression

In this stress state, principal strain ε_1 is positive and checked against limiting value given by eq. (5.10) and ε_2 is negative and checked against limiting value given by eq. (5.11).

If $\varepsilon_1 > \varepsilon_p \quad E_1 = 0$

If $\varepsilon_2 > \varepsilon_p \quad E_2 = 0$

For any of the two cases shear modulus is reduced to G and if the two principal strain $\varepsilon_1, \varepsilon_2$ exceeded the limiting values $G = 0$.

5.3.3 Compression-Compression

In this state of stress the maximum strain ε_2 is checked against limiting value given by eq.(5.8).

If $\varepsilon_2 > \varepsilon_p \quad E_1, E_2$ and $G = 0$

5.4 Computation of Unbalanced Loads

Unbalanced loads result from the assumption of linear behavior within each load increment while the true behavior is non-linear. All the sources of materials non-linearity result in equilibrium violation after a load increment and hence must be taken into account upon computing the unbalanced loads.

For each element the unbalanced forces can be calculated according to the following steps:

1- Calculate unbalanced stresses σ_{ui} from to the following expression:

$$\sigma_{ui} = ([D_{i-1}] - [D_i])\varepsilon_i \quad \text{.....5.17}$$

Where

D_{i-1}=Material stiffness matrix used in previous iteration.

D_i = Updated material stiffness matrix.

ε_i = Updated strain matrix.

2-The unbalanced forces P_{ui} corresponding to the unbalanced stresses σ_{ui} can be computed according to the following expression:

$$\{P_{ui}\} = \int_A [B]^T \{\sigma_{ui}\} dA \quad \text{.....5.18}$$

Where

$[B]^T$= transformation matrix.

5.5 Convergence Criteria

There are two most convenient methods of measuring convergence after each iteration:

unbalanced loads convergence criteria

displacement increment convergence criteria

5.5.1 Unbalanced Loads Convergence Criterion

This measure indicates the amount by which equilibrium is violated at any stage of the solution process. There are several ways by which unbalanced loads can be used as convergence measure. In this investigation the following mathematical expression is used:

$$\varepsilon = (\sum_{i=1}^{n} P_{ui}{}^{2})^{0.5} \quad \text{.....5.19}$$

This expression is known as the Euclidean norm.

Where

n= Total number of degrees of freedom.

P_{ui}= Unbalanced load per degree of freedom.

ε= Absolute error.

5.5.2 Displacement Increments Convergence Criterion

This measure assesses how close the nodal displacements and hence strains and stresses are to their correct values. In this investigation the ratio of an incremental displacement after iteration to that after a load increment of prespecified degree of freedom can be used as convergence measure:

$$\varepsilon = \frac{\delta_{ui}}{\delta_{u0}} \quad \text{.....5.20}$$

Where

δ_{ui}= Incremental displacement after each iteration.

δ_{u0}= Incremental displacement after each load increment.

ε= Percentage error.

CHAPTER(6)
APPLICATIONS AND RESULTS

This chapter demonstrates the applicability of shear resisting mechanism models and adequacy of non-linear procedure used in computer program. Modeling selected experimental deep beam does this. The analytical results are compared with their corresponding experimental results obtained by Isreal[21].

6.1 Specimen Description and Material Properties

The reinforced concrete deep beam selected for analysis in this work is one of experimental deep beams tested by Isrea1[21]. The geometry and cross sectional properties of this specimen are shown in Fig.6.1. The main longitudinal reinforcement consists of four bars of 10mm diameter with 425 N/mm^2 average yield stress. This reinforcement was placed in two layers as shown .The web reinforcement is provided by using BRC weld mesh which consists of plain bars 5.3mm diameter in both direction at 76.2mm centers. The yield stress of this of this steel is found to be 425N/mm^2. One layer of mesh is placed at each face of the specimen. The main reinforcement bars were anchored to steel blocks at their ends to prevent bond failure. To achieve this, threaded reinforcing bars were left protruding from the beam end. A 96x72x25mm steel block with holes for passing the main reinforcing bars through was embedded to each end of specimen with cement paste. Nuts were tightened to the bars at both ends.

Material properties used in this analysis are:

Uniaxial compressive strength of concrete=49.6N/mm^2

Tensile strength of concrete=3.36N/mm^2

Initial modulus of elasticity of concrete=34.7KN/mm^2

Yield strength of reinforcement=425N/mm^2

Poisson’s ratio for reinforcement=0.3

Poisson’s ratio for concrete in tension=0.3

Poisson’s ratio for concrete in compression=0.2

Concrete strain in tension=.00257

Concrete strain in compression=.0002

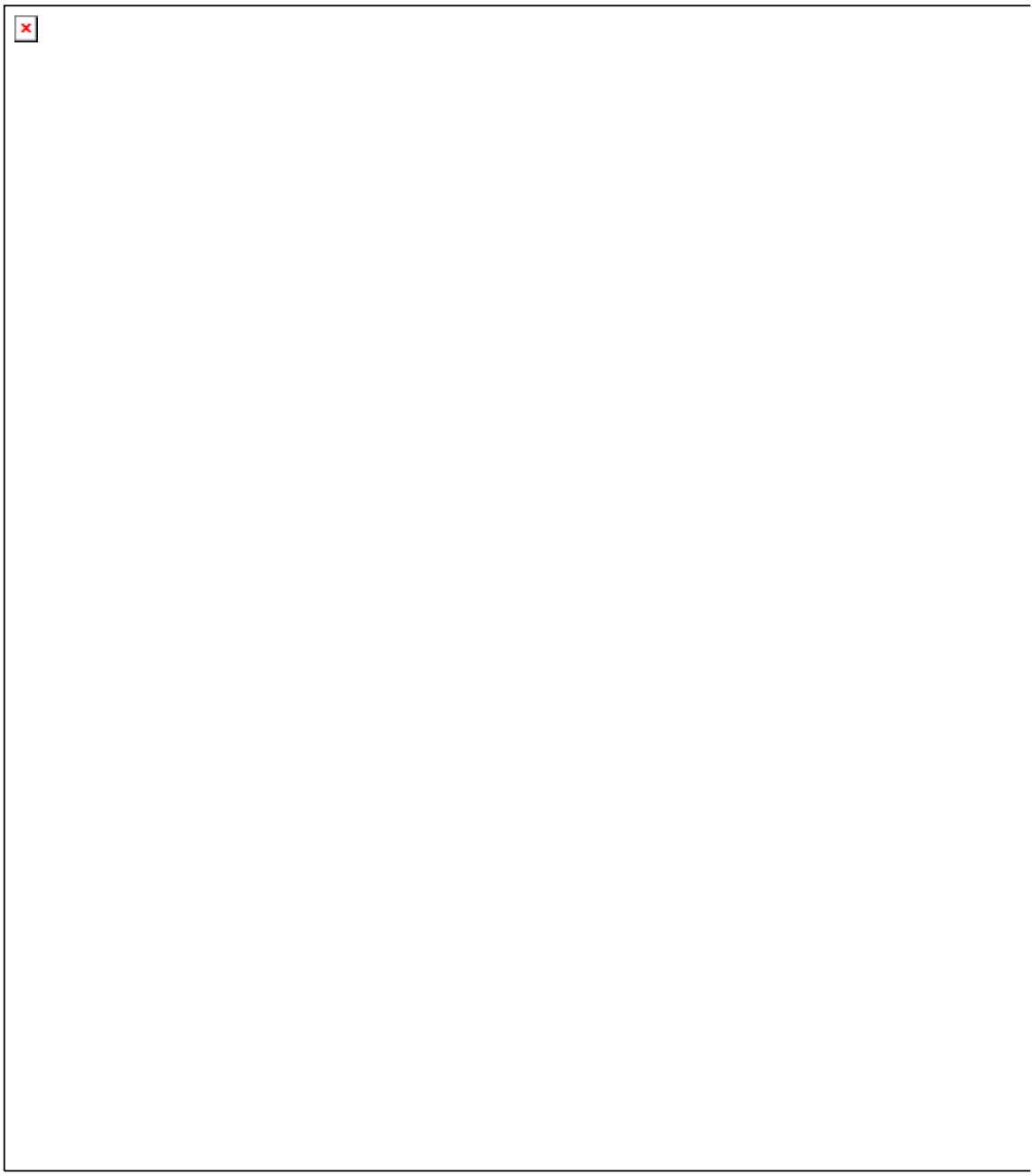

6.2 Experimental Response

Isreal[2] indicated that the first cracks occurred at an early load of 150KN within the central third span. These were flexural vertical cracks. These vertical cracks propagated quickly as the load increased, penetrating to approximately 2/3 of the depth of the beam. Next to appear at 400KN load were inclined cracks within the shear span, extending inward and towards the top third of the beam. Further inclined cracks were initiated close to the support with increasing load, and spreaded toward the loading points. At a load of 700KN,the entire section joining the supports and the loaded points was cracked and after sustaining 800KN load for short period of time, total failure occurred. Failure of the beam was typical diagonal cracking failure with final extensive crushing of the concrete between support and loading points.

The following information is obtained from experimental work of Isreal[2]:

- Crack pattern.
- Mode of failure.
- Failure load
- Load-displacement curve at center of deep beam.
- Stress distribution in vertical section.

6.3 Analytical Response

The finite element grid used to model the above deep beam is shown in Fig.6.2. The symmetry of the specimen and the applied loading permits the idealization and analysis of only one half of the beam. At the support the nodes are free to move horizontally and vertical displacement degrees of freedom are suppressed. Nodes along the centerline are permitted vertical movement only and the horizontal degrees of freedom are

suppressed in order to satisfy the condition of symmetry. Idealization of concrete required 77 modified quadrilateral elements as shown in Fig.6.2 (a). Layout of reinforcement discretization is shown in Fig.6.2 (b). The main reinforcement bars are concentrated in two layers. 12 flexural line elements are used to idealize them. The web reinforcement is represented by one-dimensional axial bar elements and 114 such elements are used for this purpose. The bond slip along the concrete-main reinforcement interface is modeled by defining double nodes with coinciding coordinates along the interface. 12 fictitious springs (dimension less) are used to connect the concrete and steel. The layout of the link elements discretization is shown in Fig.6.2(c). Link elements number 1 and 7 are assigned very high stiffness values to produce the effect of hooks near support.

The discretization of the member according to the above-mentioned pattern led to 112 nodal points; all but 12 have two translation degrees of freedom each. The 12 nodes connecting the main reinforcement element have, in addition to translation degrees of freedom, a rotational degree of freedom permitted in each.

The load is applied at nodes 109,110 and 111. The load is divided into increments, which are applied in percentage of failure load.

The vertical displacements at the centerline obtained from analysis at various load levels are plotted, along with experimental displacements as shown in Fig.6.3. Comparison between the two curves indicates a good agreement between the analytical and experimental results.

One of the important advantages of the finite element method is its ability to provide a complete description of the Stress State at any section of the beam and at any load level.

In this analysis the computer output included such information, and three types of stress distributions at various load level are presented. These are:

a) Longitudinal stresses in the two layers of the main reinforcement as shown in Fig.6.4 (a) and Fig6.4 (b). These are plotted at three different load levels. It is evident that the stresses are increased as the applied load is increased. None of the reinforcement segments reached the yield limit at failure load level, which is caused by crushing of concrete over support (diagonal crack failure). We indicated this mode of failure by crushing of the following concrete elements:
8,9,16,17,24,25,31,32,38,39,46,47,53,54,62,63,69,70,76,77.

b) The computer analysis also provided the bond stresses in the bond links as shown in Fig.6.5 (a) and Fig.6.5 (b). These are plotted at two load levels. Link 1 and 7 were assigned very high stiffness values to reproduce the effect of hooks near the support. The bond stress intensity showed characteristic peaks at links 3 and 9. It is clear that no bond failure had occurred as it is evident from these plots. Where bond stresses in all the links remained below the maximum bond stress capacity.

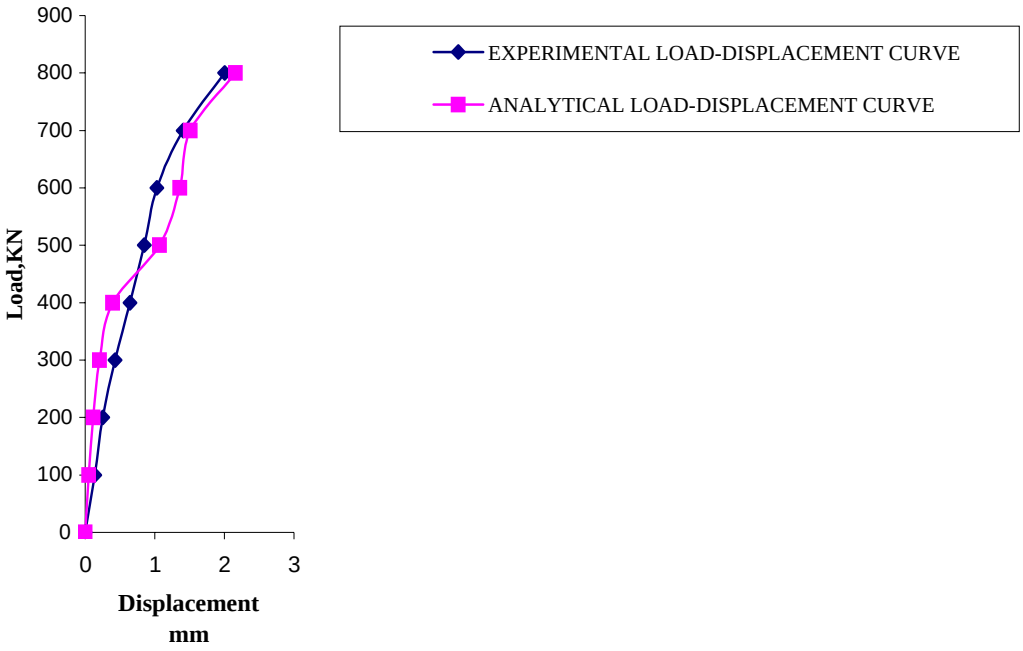

Fig.6.3 Comparison Between Experimental and Analytical Load-Displacem Curve

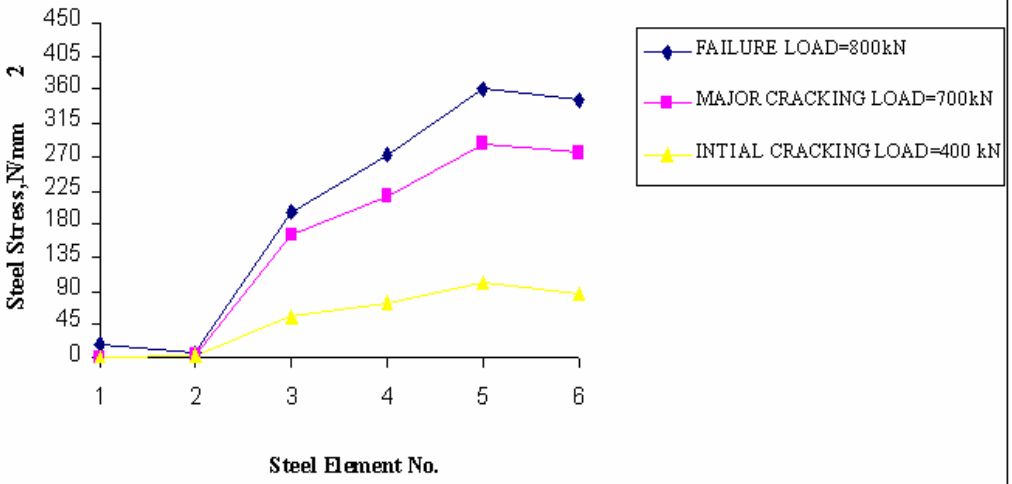

Fig.6.4(a) Effect of Load in Main Reinforcement Stresses (Lower Layer)

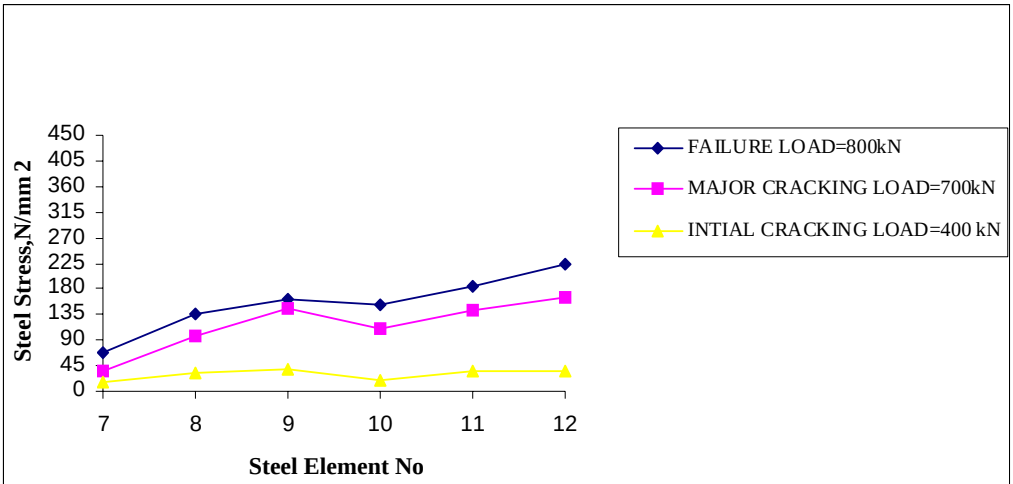

Fig.6.4(b) Effect of Load in Main Reinforcement Stresses (Upper Layer)

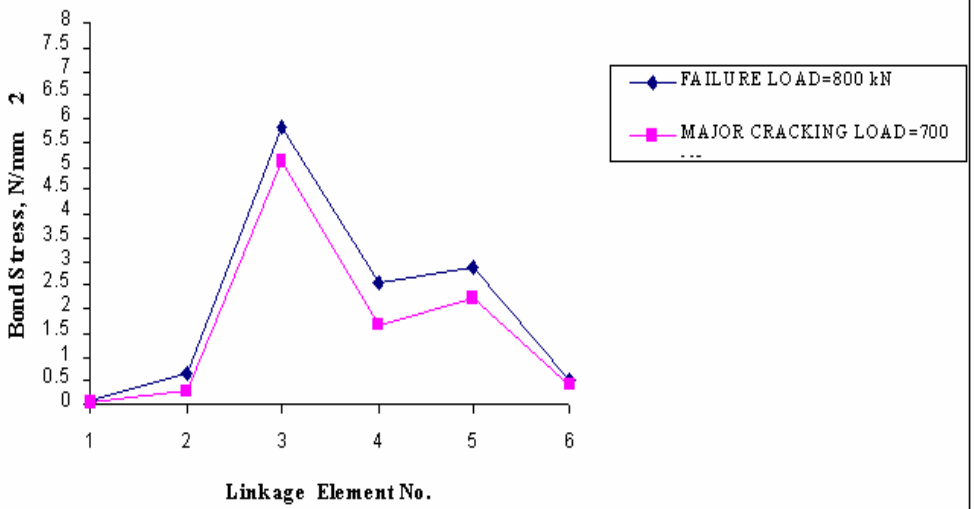

Fig.6.5(a) Effect of Load in Bond Stress Lower Layer

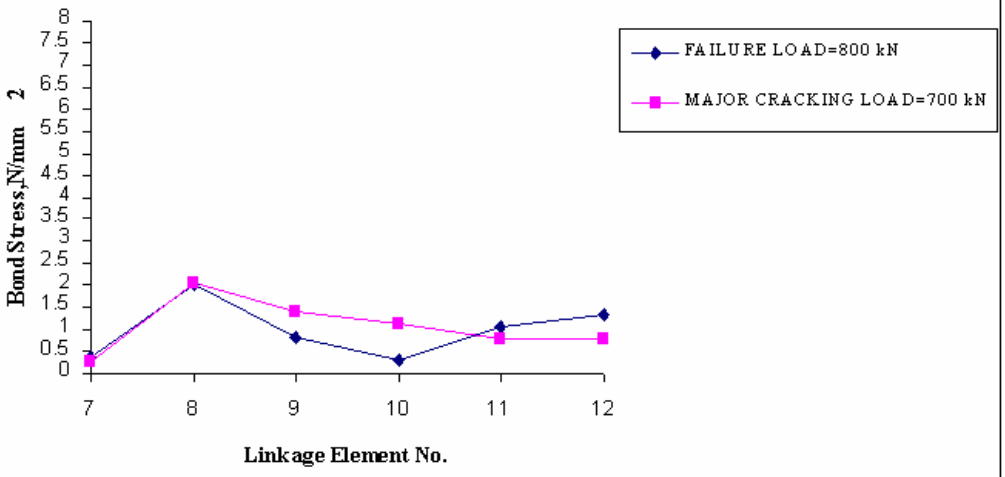

Fig.6.5(b) Effect of Load in Bond Stress (Upper Layer)

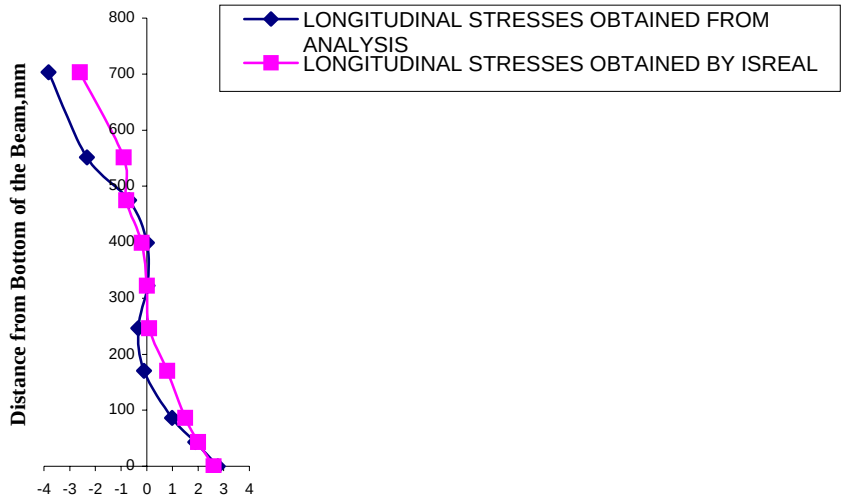

Fig.6.6 Comparison Between Experimental and Analytical Longitudinal Stresses at Centre of Span

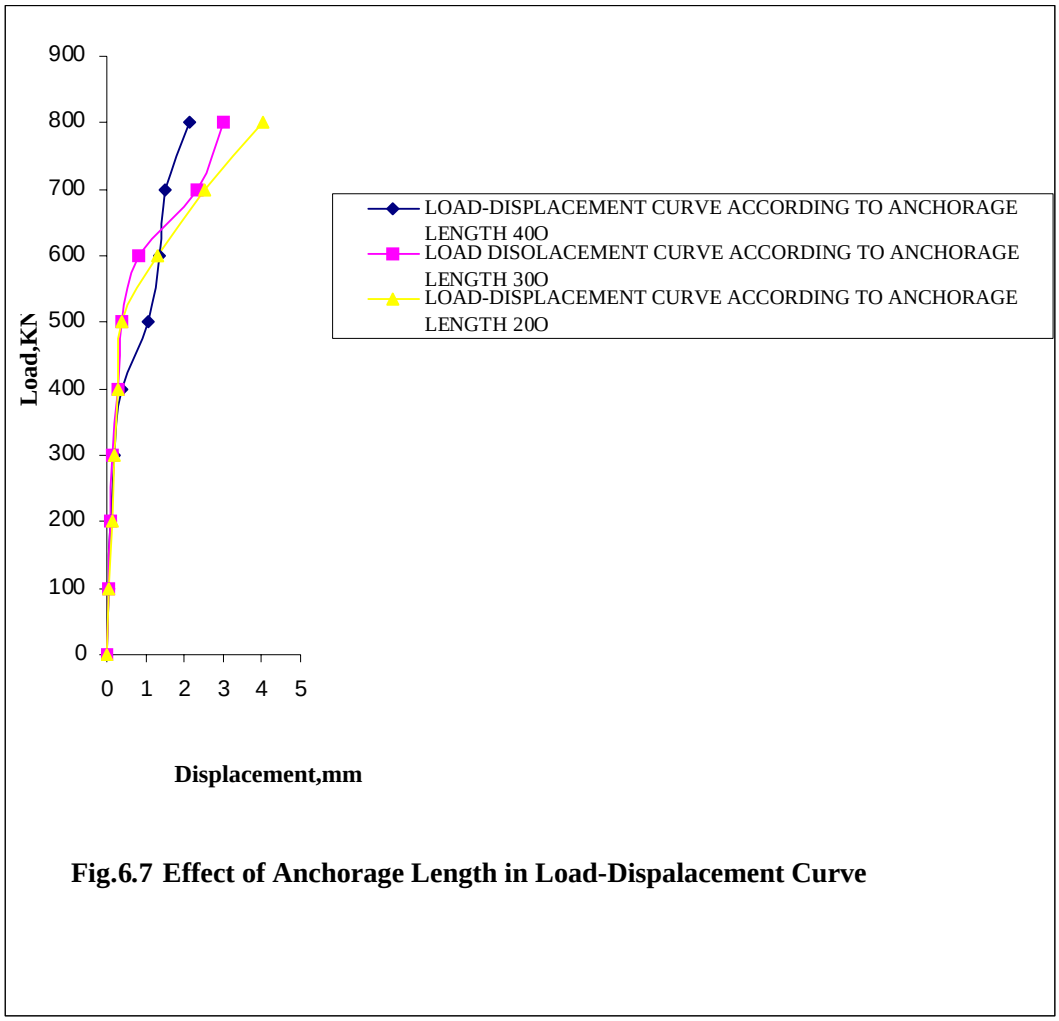

Fig.6.7 Effect of Anchorage Length in Load-Dispalacement Curve

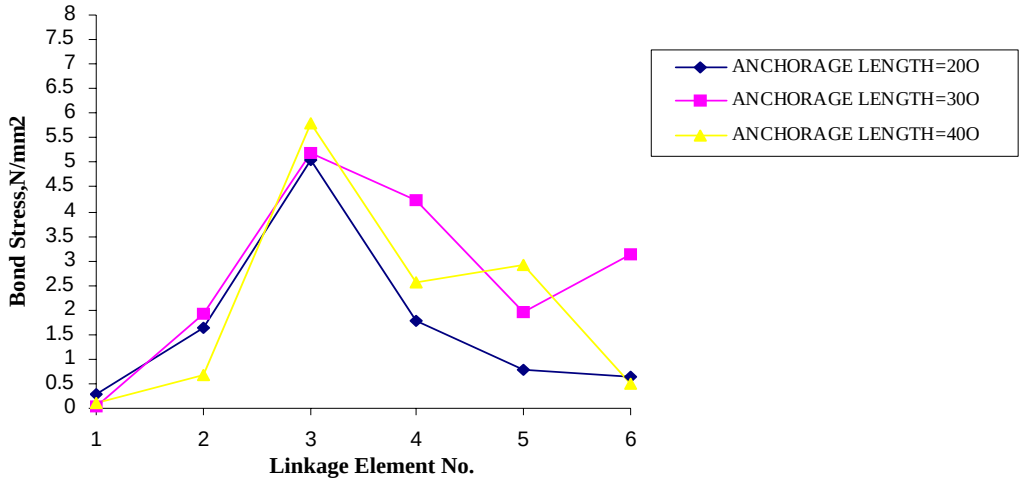

Fig.6.8 (a) Effect of Anchorage Length in Bond Stress (Lower Layer)

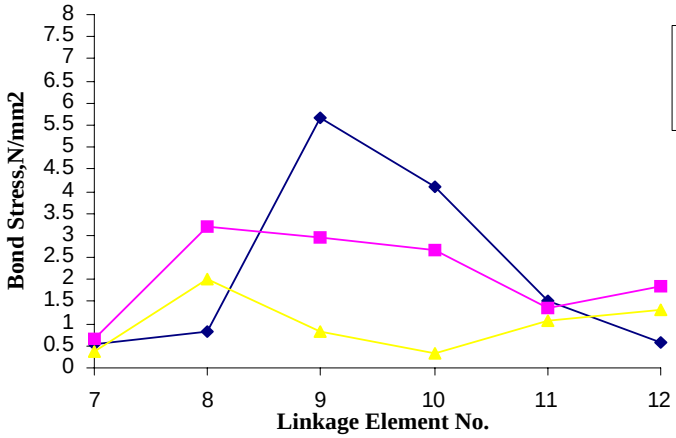

Fig.6.8 (b) Effect of Anchorage Length in Bond stress (Upper Layer)

6.4 Conclusions

Based on the application of the analytical model the following conclusions is drived:

1-In reinforced concrete deep beams the effect of material non-linearity can not taken into account in load-displacement curve up to elastic limit. This is clear from the fact that diagonal crack

does not occurred below the elastic limit.

2-Stresses in main longitudinal reinforcement increases toward the mid-span but none of the reinforcement segments reach the yield limit. This is indicated from the formation of flexural cracks near mid span but this crack is not propagated above the elastic limit (flexural failure is not occurred for reinforced concrete deep beams).

3-The bond stress in R.C deep beams with proper hooking at support increases with increasing the load.

4- In R.C deep beams the effect of anchorage length (hooking) at support is taken into account after the diagonal cracking takes place (above the elastic limit).

5- Increasing of anchorage length results in reduction of vertical displacement and decreasing in bond stress.

6.5 Note

In this analysis it is clear that bond-slip mechanism seems to take the major part of shear transfer while the other mechanisms aggregate interlock and dowel action take less part. This is clear from the close relation-ship between the experimental and the analytical results obtained by considering bond-slip mechanism

only. This confirm the conclusion reached by task committee 426 on shear and diagonal tension [1], that in reinforced concrete deep beams most of the load is transmitted to the support by arch action and not transmitted tangential force to the nearby parallel plane and thereby reduces the contribution of other types of shear transfer mechanism aggregate interlock and dowel action.

6.6 Further Work

In this research only the effect of bond-slip mechanism is taken into account in the application of computer program for non-linear problem therefor its recommended to make applications of such problem considering the effect of aggregate interlock and dowel action mechanisms and study the contribution of each mechanism in shear capacity of reinforced concrete deep beams.

References:

1-Task committee 426 on shear and diagonal tension of the committee on masonry and reinforced concrete, Journal of the structural division, 1973.

2- Isreal Besser Avila “Strength of Slender reinforced concrete Walls”, Ph.D dissertation university of Leeds,1983.

3-Dulascska, H., “Dowel action of reinforcement crossing cracks in concrete”, ACI Journal,1972.

4- Fenwick, R.C., and Paulay, T.,"Mechanism of shear resistance of concrete beams", Journal of structural division, ASCE, 1968.

5- De Pavia,H.A.R. and siess,C.P.”Strength and Behaviour of deep beams in shear”, ASCE Journal, 1965.

6- Gergely, P.,”Splitting cracks along the main reinforcement in concrete members", research report, Department of structural engineering, Cornell university, 1969.

7-Taylor, H.P.J.,” Investigation of forced carried across cracks in reinforced concrete beams in shear by interlock of aggregate", Cement and concrete association,London,1970.

8- Paulay,T.,and Lober,P.J.,"Shear transfer by aggregate interlock", ACI Journal,1974.

9-Kong et al, P.J ”Web reinforcement effects on deep beams", the structural engineer vol.50 No.11,1972.

10- Kong, F.K. and Robins, P.J “Deep Beams with Inclined Web Reinforcement", ACI Journal,1972.

11-Kong, F.K. and Robins, P.J ”Web reinforcement effect on light weight concrete deep beams", ACI Journal,1971.

12- Kong, F.K. and Robins, P.J"Web reinforcement effect on deep beams”, ACI Journal ,1972.

13 - Smith and Vantsiotis, A.S.”Shear strength of deep beams" ACI Journal,1982.

14- Kang Hai tan, “Shear behavior of large reinforced concrete deep beams”, ACI Journal,1999.

15- Ashraf, ”Tests of reinforced concrete continuos deep beams”, ACI Journal,1997.

16- Kang Hai tan ,”Main tension steel in high strength reinforced concrete deep beams”, ACI Journal,1997.

17- Houde and Merza, M.S.,”Afinite element analysis of shear strength of reinforced concrete beams", ACI Journal,1974.

19- Ngo,D. and Scordelis, A.C.,”Finite element analysis of reinforced concrete beams", ACI Journal,1967.

20- Nilson, “Internal measurement of bond slip”, ACI Journal, 1967

21- Ngo, D.,Franklin, H.A., and scordelis, A.C.,” Finite element study of reinforced concrete beams with diagonal tension crack",UC SESM report no.70-19 university of clifornia,1970.

22- Franklin, H.A.,”non linear analysis of reinforced concrete frames and panel, Ph.D Dissertation University of berkeley,1970.

24- Liu,C.Y.,Nilson,A.H., and Slate, F.O.,"Biaxial stress-strain relation-ship for concrete”, Journal of structural divission,1972.

25- Tasuji,M.E.,Nilson, A.H., and Slate,F.O.,”The behavior of plain concrete subject to biaxial stress”, report of structural engineering,Cornelluniversity1976.

26- cedolin, L. and Dei Poli, “Finite Element Non-linear Plane stress Analysis of reinforced concrete”, costruzioni in cemento armato,1976.

27- CIRIA Guide 2 “ The Design of Deep Beams in Reinforced Concrete”, Construction Industry Research and Information Association, London, 1977.

28- Committee European du Beton “Internationa recommendations for the design and construction of concrete structures, principles and recommendations”, Proceedings of the Sixth F.I.P , 1970 , Prague - Czechoslovakia.

29- ACI Committee 318 “Building Code Requirements for Reinforced Concrete”, American Concrete Institute , Detroit, Michigan, 1999.

ملخص

إن الغرض من هذا البحث هو تحليل العارضات العميقة في الحالة الخطية،اللاخطية وحـالة التحميل القصوى.

استخدمت طريقة العناصر المحددة لدراسة سلوك العارضات العميقة تحت تأثير الأحـمال المتزايدة مع الأخذ في الاعتبار كل العوامل الرئيسية المسببة للاخطية. يوضح هذا البحث جـميع الاعتبارات الأولية المستخدمة لتمثيل آليات نقـل قوى القص المختلـفة ترابط الركام،الفعل الوتدى وانزلاق الترابط بين الخرسانة وحديد التسليح.

المعادلات المستخدمة لتمثيل آلية ترابط الركام مستنبطة من نماذج تحليلية مرتبطة ببيانات معملية لإيجاد إجهاد وجساءة القص لأعضاء نابضة خاصة استخدمت لتمثيل هذه الآلية.هذه المعادلات كتبت بدلالة عرض الشق، مقاومة الخرسانة وإزاحة القص.اتبعت نفس الطريقة لتمثيل آلية الفعل الوتدى وكتبت المعادلات الخاصة ذه الآلية بدلالة قطر حديد التسليح، إجهاد الخضوع وإزاحة الوتد ومقاومة التهشيم للخرسانة.

التلاحم بين الخرسانة وحديد التسليح تم حسابه باستخدام عضو نابض صفرى الأبعاد، جساءة القص لهذا العضو تم حسا ا من معادلات تستند على بيانات معملية.

استخدمت عناصر رباعية الأضلاع وأخرى مثلثية لتمثيل الأعضاء الخرسانية مع اعتبار أن الخرسانة مادة مختلفة الخواص لها جساءة ساسية مستنبطة من علاقة الإجهاد والانفعال للخرسانة تحت تأثير الحالة الثنائية العامة للإجهاد.

تم تمثيل حديد التسليح في صورة أعضاء موصلة لنظام عقدى حيث تم استخدام أعضاء ذات بعد واحد تعمل كعناصر قابلة للانحناء وأخرى محورية مع افتراض أن حديد التسليح مادة مرنة كاملة اللدونة.